

Suspended-load experiments in a curved  
flume, run no. 6

A.M. Talmon and J. de Graaff

report no. 5-91, August 1991

part of:

STW-project; River bend morphology with suspended sediment.

Delft University of Technology  
Faculty of Civil Engineering  
Hydraulic Engineering Division

## ABSTRACT

A laboratory experiment in a 180 degree curved flume with a mobile bed and suspended sediment transport is reported. The flow is steady.

The bed topography is measured by means of a profile indicator. Free and forced alternating bars are present. The steady part of the bed topography, which is forced by curvature, is characterized by a below critical response of the transverse bed slope. Downstream of the bend entrance overdeepening occurs, this is repeated with a somewhat smaller amplitude further downstream. Suspended sediment concentrations are measured.

<u>CONTENTS</u>		page
ABSTRACT		3
1.	INTRODUCTION	10
2.	THE LABORATORY EQUIPMENT	
2.1.	The flume	11
2.2.	Measuring equipment	
2.2.1.	Discharge measurement	11
2.2.2.	Slope and depth measurements	12
2.2.3.	Concentration measurement	12
2.3.	Measuring procedure	13
3.	FLOW AND SEDIMENT CONDITIONS	
3.1	Free and forced bars during bend measurements	14
3.2.	The sediment	
3.2.1.	Sieve curve	14
3.2.2.	Fall velocity	15
3.3.	Flow conditions	15
4.	RESULTS	
4.1.	Depth measurements	
4.1.1.	Mean depth	17
4.1.2.	Bed form statistics	17
4.2.	Concentration measurements	18
5.	DISCUSSION	
5.1.	Introduction	20
5.2.	The Z parameter	20
5.3.	Percentage of suspended sediment transport	21
5.4.	Transport formulae	22
5.5.	Bed-shear stress and sediment transport	25
5.6.	Adaptation lengths	27
5.7.	The bed topography	28

5.8.	Comparision with a straight flume experiment	28
6.	CONCLUSIONS	29
	REFERENCES	30

APPENDIX A Ensemble averaged water depth data

APPENDIX B Concentration data

APPENDIX C Free bars

FIGURES

LIST OF TABLES

3.1a	Measured parameters	16
3.1b	Calculated parameters	16
4.1	Parameter sets of the equilibrium concentration profile	19
5.1	Percentage of suspended sediment transport	22
5.2	The mobility parameter B	26
5.3	Interaction parameters of analytical model	29

LIST OF FIGURES

1	Layout, Laboratory of Fluid Mechanics curved flume
2	Sieve curve of sediment
3	Probability density distribution of fall velocity
4	Longitudinal water level slope
5	Contour lines of the relative water depth $a/a_0$
6	Longitudinal profile of the water depth
7a..1	Water depth in cross-direction
8a	Probability distribution of bed level, cross-section 1...5
8b	Probability distribution of bed level, flume axis
9	Concentrations at cross-section 1 and curve fit by Rouse profile
C1...4	Positions of bars

LIST OF SYMBOLS

a	local ensemble mean water depth	[m]
a'	local fluctuation of bed level	[m]
a <sub>0</sub>	mean water depth of cross-section 1 to 5 (in earlier reports: mean depth at cross-section 1)	[m]
$\hat{a}$	complex amplitude of bed oscillation	[-]
A	critical mobility number	[-]
B	mobility parameter; $B = \tau_{cr}/(\mu\tau)$	[-]
c	local concentration	[g/l]
c <sub>r</sub>	concentration at reference level	[g/l]
$\bar{c}$	local depth averaged concentration	[g/l]
$\bar{c}_{tr}$	total transport concentration; $\bar{c}_{tr} = Q_s/Q_w \cdot 10^{-3}$	[g/l]
$\bar{c}_{trb}$	transport conc. of bed-load; $\bar{c}_{trb} = S_{s \text{ bed}}/(\bar{u}a_0) \cdot 10^{-3}$	[g/l]
$\bar{c}_{trs}$	transport conc. of suspended-load; $\bar{c}_{trs} = S_{s \text{ sus}}/(\bar{u}a_0) \cdot 10^{-3}$	[g/l]
C	parameter in Ackers White formula	[-]
C	Chézy coefficient, with $d=a_0$ ; $C = \bar{u}/\sqrt{(di)}$	[m <sup>0.5</sup> /s]
d	a representative water depth	[m]
D <sub>gr</sub>	dimensionless grain diameter; $D_{gr} = D_{50}(\Delta g/\nu^2)^{1/3}$	[-]
D <sub>g</sub>	geometric mean grain diameter; $D_g = \sqrt{(D_{84}/D_{16})}$	[m]
D <sub>p</sub>	grain size for which p% of the grains is smaller than D <sub>p</sub>	[-]
D <sub>50</sub>	median grain size	[m]
D <sub>s</sub>	sedimentation diameter	[m]
F <sub>g</sub>	grain Froude number	[-]
F <sub>g0</sub>	critical grain Froude number	[-]
F <sub>gr</sub>	grain mobility number	[-]
Fr	Froude number, with $d=a_0$ ; $Fr = \bar{u}/\sqrt{(gd)}$	[-]
G	coefficient in gravitation term	[-]
H	depth of the flume	[m]
i	water surface slope	[-]
k	complex wave number	[1/m]
k <sub>b</sub>	wave number in transversal direction	[1/m]
k <sub>sn</sub>	secondary flow convection factor	[-]
L <sub>c</sub>	arc length of the bend	[m]
L <sub>cs</sub>	length scale of adaptation of concentration	[m]
m	parameter in Ackers White formula	[-]
n	parameter in Ackers White formula	[-]
n	coordinate in transverse direction	[m]

P	wetted perimeter	[m]
$Q_w$	water discharge	[m <sup>3</sup> /s]
$Q_s$	sediment discharge	[g/s]
$r_u$	profile function of the velocity profile	[-]
$r_c$	profile function of the concentration profile	[-]
$R_c$	radius of curvature of axis of flume	[m]
$R_g$	grain Reynolds number; $R_g = \sqrt{(gD_{50}^3)/\nu}$	[-]
s	coordinate in streamwise direction	[m]
$S_{s \text{ sus}}$	transport rate of suspended sediment, per unit width, in s-direc.	[g/m/s]
$S_{n \text{ sus}}$	transport rate of suspended sediment, per unit width, in n-direc.	[g/m/s]
$S_{\text{tot}}$	total transport rate, per unit width	[g/m/s]
T	water temperature	[°C]
u	local depth averaged mean flow velocity	[m/s]
$\bar{u}$	overall averaged mean flow velocity: $\bar{u} = Q_w/(Wa_0)$	[m/s]
$u_{\text{cr}}$	critical depth averaged velocity	[m/s]
$u_*$	bed friction velocity, based on C : $u_* = (u/g)/C$	[m/s]
W	width of the flume	[m]
$w_s$	fall velocity of sediment	[m/s]
Z	the Z parameter: $Z = w_s/(\beta\kappa u_*)$	[-]
$z_r$	reference level	[m]
$z_s$	surface level	[m]
$\beta$	ratio of exchange coefficients of sediment and momentum	[-]
$\beta$	coefficient in the bed shear-stress direction model	[-]
$\kappa$	von Karman constant	[-]
$\lambda_c$	adaptation length of concentration	[m]
$\lambda_s$	adaptation length of bed level	[m]
$\lambda_{\text{sf}}$	adaptation length of bed shear-stress	[m]
$\lambda_w$	adaptation length of velocity	[m]
$\mu$	efficiency factor	[-]
$\rho$	density of water; $\rho = 1000 \text{ kg/m}^3$	[kg/m <sup>3</sup> ]
$\rho_s$	density of sediment; $\rho_s = 2650 \text{ kg/m}^3$	[kg/m <sup>3</sup> ]
$\sigma_g$	gradation of sediment; $\sigma_g = D_{84}/D_{16}$	[-]
$\tau$	total drag	[N/m <sup>2</sup> ]
$\tau'$	effective grain-shear stress; $\tau' = \mu\tau$	[N/m <sup>2</sup> ]
$\tau_{\text{cr}}$	critical bed-shear stress	[N/m <sup>2</sup> ]

$\nu_{tm}$	turbulent diffusion coefficient of momentum	[m <sup>2</sup> /s]
$\nu_{tc}$	turbulent diffusion coefficient of mass	[m <sup>2</sup> /s]
$\theta$	Shields number, with $d=a_0$ : $\theta = di/(\Delta D_{50})$	[-]
$\theta_{cr}$	critical Shields number	[-]
$\Delta$	relative density of sand; $\Delta = 1.65$	[-]

## 1. INTRODUCTION

The project at hand is directed towards the computation of river bend morphology in case of alluvial rivers transporting a significant part of their bed material in suspension.

The bed topography and local concentrations of suspended sediment are measured. The objective of the experiment is to provide data on the morphology of river bends which are characterized by a system response near the point of zero damping. Such an experiment has recently been realized in a straight channel at Delft Hydraulics, Ahmed (1990), Talmon & De Graaff (1991). The choice of the parameters values of the present experiment is guided by the values of that straight channel experiment.

In chapter 2 the laboratory equipment is described briefly. In chapter 3 the experimental conditions are given. In chapter 4 the results of the measurements of bed topography and concentration are reported. In chapter 5 the results are discussed. In chapter 6 the conclusions are presented.

This research is a part of the project: 'River bend morphology with suspended sediment', project no. DCT59.0842. The project is supported by the Netherlands Technology Foundation (STW).

## 2. LABORATORY EQUIPMENT

### 2.1 The flume

The layout of the LFM curved flume is shown in figure 1. Water is pumped from an underground reservoir to an overhead tank and led to the flume. The water discharge is controlled by a valve in the supply pipeline. The sand supply is effectuated by thirteen small holes of 2.5 mm diameter, in the bottom of a container located 0.5 m above the water surface.

After passing the tailgate of the flume, by which the water level is governed, the water pours in a settling tank. After passing this tank the water flows back into the underground reservoir.

The dimensions of the flume are:

inflow section length	13.00 m
outflow section length	6.70 m
arc length of the bend	$L_c = 12.88$ m
radius of the bend	$R_c = 4.10$ m
width of the flume	$W = 0.50$ m
depth of the flume	$H = 0.30$ m

The bottom of the flume and the side walls of the straight section are made of glass. The side walls of the curved section are made of perspex.

### 2.2 Measuring equipment

#### 2.2.1 Discharge measurement

-----

The discharge is controlled by a valve in the supply pipeline. The discharge is measured by a volumetric method. A 150 liters barrel is partly filled during about 30 seconds at the downstream end of the flume. The volume is measured and divided by the filling time.

### 2.2.2 Slope and depth measurements

-----

The measurements of the bottom are performed with an electronic bed profile indicator (mini-PROVO) and gauges attached to the side walls of the flume (interval 4 m) to measure the water levels. From these measurements the longitudinal slope of the water level and the local depth are calculated. The profile indicator is traversed in cross-sectional direction. In each cross-section 9 equidistant measuring points are used. The carriage in which the PROVO is mounted is also traversed in longitudinal direction. In longitudinal direction 48 cross-sections are situated, these are indicated in figure 5. The distance between these cross-sections at the flume axis is 0.32 m. The profile indicator is moved continuously in cross-sectional direction, this is controlled by electronic hardware. The position of the profile indicator is measured electronically. The carriage is moved manually in longitudinal direction.

### 2.2.3 Concentration measurements

-----

Sediment concentrations are measured at cross-section 1. They are determined by siphoning. Measuring periods of about 45 minutes are employed.

### 2.3 Measuring procedure

The flume is partly filled with sand. The thickness of the sand bed at the entrance of the flume is 0.16 m, at the exit the bed thickness is about 0.04 m.

The sand supply is measured by weighing the contents of the supply container. The sand settled in the settling tank is gathered at regular intervals (about 24 hours) and is weighed under water. The results are converted to equivalent weights of dry sand. The supply rate is adjusted such that the supply rate and the discharge rate balance.

The water levels are measured daily.

In the initial phase of the experiment the longitudinal bed slope and the flow rate were adjusted to yield the desired physical parameters. The objective was to yield the same water level slope as the prepared bed, at a desired waterdepth. After some days this seemed to be succeeded. From then on the controls remained untouched and the experiments started:  $t=0$ .

At  $t=40$  hours, the measurement of bed topography and concentrations started. At that time no significant changes of the water levels were measured. In and outflow of sand were also nearly equal. The measurements ended at  $t=100$  hours.

The stationary bed topography is obtained by ensemble averaging of 23 bed level measurements. The time interval between water level measurements is about 2 hours. The interval between bed level measurements is 2...3 hours.

Each bed level measurement consists of 48 cross-sectional traverses. Within a cross-section 9 measuring points are used. The data are digitized by an APPLE data-acquisition system. A900 HP mini computer is used to store the data. Further the data are processed by a central main frame IBM computer of the Delft University. The longitudinal slope is determined from the water levels.

### 3. EXPERIMENTAL CONDITIONS

#### 3.1 Free and forced bars during bend measurements

In the experiment free and forced alternating bars are present. The free bars are inherent of the system. The forced bars are forced by an external boundary condition. Which in this case is the curvature of the flume. At the entrance of the flume a tendency to develop forced bars was noticed.

It is tried to eliminate this forced bar formation by preventing sand to accumulate near the sand feeder. When some sand started to accumulate it was smoothed out by hand. This way it appeared possible to keep the bed flat up to  $\approx 3$  m downstream of the sand feeder. From this location on, which is still in the straight channel, free bars started to develop and migrate downstream. The bars continued to migrate down to the channel exit. The wave length of the free bars is: 4.9 m, their celerity is 0.35 m/h, (appendix C). The steady forced bars in the bend, which are forced by curvature, are determined by ensemble averaging of bed level measurements to filter out free bar contributions.

#### 3.2 The sediment

##### 3.2.1 Sieve curve

-----

At the end of the experiment sediment samples were collected from three different sources: the sand supply container, the upper layer of the bed and sediment which is transported in suspension. Figure 2 shows the cumulative probability density distributions of the grain sizes of these sediment samples. Characteristic grain diameters are:

	$D_{10} [\mu\text{m}]$	$D_{16} [\mu\text{m}]$	$D_{50} [\mu\text{m}]$	$D_{84} [\mu\text{m}]$	$D_{90} [\mu\text{m}]$	$D_g [\mu\text{m}]$	$\sigma_g$
bed layer	81	84	105	142	>150	109	1.69
supply cont.	77	81	94	115	124	97	1.42
suspended sed.:	77	81	94	115	124	97	1.42

The quantity  $D_p$  is defined as the grain size for which p % of the total mixture volume is smaller than  $D_p$ .

The geometric mean diameter is defined by:  $D_g = \sqrt{(D_{84} D_{16})}$

The gradation of the sediment is defined by:  $\sigma_g = D_{84}/D_{16}$   
 These results indicate that some grain sorting has taken place during the course of the experiments. The sediment of the bed layer has a relatively large number of coarse particles.

### 3.2.2 Fall velocity

-----

The fall velocity of suspended-sediment is determined in a settling tube. This is a device to determine the fall velocity distribution of particles in a sample. At the lower end of the settling tube the sediment particles accumulate on a very sensitive weighing device. A cumulative weight distribution of the sample as a function of the measuring time is obtained. This distribution is converted into the fall velocity distribution of the sample using the height of the settling tube (Slot and Geldof, 1986).

The sample of suspended-sediment is siphoned at about 1 m upstream of cross-section 1. It is siphoned at the centre-line 2 cm below the water level. The sediment is gathered during 22 hours. The samples are dried and split into amounts that can be used in the settling tube.

Figure 3 shows the probability distribution of the fall velocity of sediment originating from the supply container.

The mean fall velocity, at 20°C, of sediment originating from the supply container is:  $w_s = 0.0085$  m/s. The mean fall velocity, at 20°C, of suspended-sediment is:  $w_s = 0.0081$  m/s. At higher temperatures the fall velocity increases; 2% per °C. The sedimentation diameter is:

$$D_s = 100 \mu\text{m}.$$

### 3.3 Flow conditions

The flow conditions are given in table 3.1a and 3.1b. The values of parameters determined by measurement are given in table 3.1a. The values of parameters obtained by calculation are given in table 3.1b.

Table 3.1a Measured parameters

$Q_w = 0.0039$	$[m^3/s]$
$W = 0.50$	$[m]$
$a_0 = 0.038$	$[m]$
$i = 4.6 \cdot 10^{-3}$	$[-]$
$D_{50} = 94$	$[\mu m]$
$w_s = 8.1 \cdot 10^{-3}$	$[m/s] (20^{\circ}C \text{ susp.})$
$Q_s = 6.4$	$[g/s]$
$T = 18.0$	$[^{\circ}C]$

Table 3.1b Calculated parameters

$\bar{u} = Q_w / (W a_0)$	$= 0.200$	$[m/s]$
$\bar{c}_{tr} = (Q_s / Q_w) 10^{-3}$	$= 1.64$	$[g/l]$
$C = \bar{u} / \sqrt{(a_0 i)}$	$= 14.9$	$[m^{0.5}/s]$
$Fr = \bar{u} / \sqrt{(g a_0)}$	$= 0.32$	$[-]$
$\theta = a_0 i / (\Delta D_{50})$	$= 1.16$	$[-]$
$u_* = (\bar{u} / g) / C$	$= 0.042$	$[m/s]$
$D_s = 100$	$[\mu m]$	$(\text{susp.}, \text{sec. 3.1.2})$
$Z = w_s / (\beta \kappa u_*)$	$= 0.28$	$(\text{sec. 4.2.2})$

#### 4. RESULTS

##### 4.1 Depth measurements

###### 4.1.1 Mean depth

-----

The ensemble relative water depth of the 23 measuring sessions are tabulated in appendix A. Figure 5 shows the ensemble-averaged contour line map of the relative water depth (normalized with the mean water depth of cross-section 1 to 5). The contour lines are drawn at intervals of  $\Delta a/a_0 = 0.2$ . The relative depth, at 0.3 W, 0.5 W and 0.7 W, as a function of longitudinal distance is depicted in figure 6. Figures 7a to 7l show the ensemble averaged flow depths of each cross section.

A point-bar and associated overdeepening occurs in the region of cross sections 12 to 19. This is repeated in the region of cross-sections 41 to 45 but with a somewhat smaller amplitude. Consequently the wave length of stationary oscillation is about 9 m.

###### 4.1.2 Bed-form statistics

-----

The bed consists of free bars and ripples which move downstream. The ripple height is a significant fraction of the flow depth. The ripples cause a significant form drag to the flow. This is reflected in the low Chézy value;  $C = 14.9 \text{ m}^{0.5}/\text{s}$ . The large dimensions of the bed-forms also affects the choice of reference level, i.e. the level above which sediment is considered to be transported as suspended load and below which the sediment is considered to be transported as bed-load. To guide the choice of reference level the probability distribution of bed-form height is calculated. This is only possible at the channel centre-line because at other locations free bars will also be included. The data of individual local depth measurements is gathered and normalized with their local ensemble-averaged value:  $a'/a$ . (at each location 23 data points are available, the total number is 1104)

The probability distribution is given in fig.8. Also the distribution in the entrance channel is given, here also data off-centre line is considered. The distribution at centre-line is indeed somewhat narrower. In fig.8 the 5% and 10% exceedance levels are indicated. At the centre-line these are within the range: 0.3...0.35a.

#### 4.2 Concentration measurements

The concentrations are measured at the channel centre-line at cross-section 1, fig 9. The measurements are used to establish the values of parameters of the concentration vertical at equilibrium conditions. The Rouse concentration-profile is fitted with the measurements. This profile is based on a parabolical function for the turbulent exchange coefficient over the vertical.

The parameters of the concentration vertical are:

- the reference height  $z_r/a$
- the concentration at reference height  $c_r$
- the Z parameter,  $w_s/(\beta\kappa u_*')$

The concentration-profile is given by:

$$c = c_r \left( \frac{z_r}{a_0 - z_r} \frac{a_0 - z}{z} \right)^Z \quad (4.1)$$

Curve fitting has been performed with the aid of a computer program which, given  $z_r$ , estimates the Z and  $c_r$  parameter values of eq.(4.1). A least squares method is employed. Data points at  $a < 0.35a_0$  and some values larger than 3.5 g/l, presumably caused by ripples are discarded. The results are given in table 4.1. A curve fit of the concentration data at cross-section 1 is included in fig. 9, a reference height of  $z_r/a_0 = 0.25$  is applied.

Table 4.1 Parameters of the equilibrium concentration-profile

$z_r/a_0$ [-]	$c_r$ [g/l]	Z [-]	$\bar{c}$ [g/l]
0.25	2.7	0.28	1.70

The estimated Z parameter value of the concentration vertical is: Z=0.28. The reference concentration will vary with the choice of

the reference level. The depth-averaged concentration given in table 4.1 is the integral of the concentration curve eq. (4.1) , section 4.2.3. The average value of data points,  $z_r/a > 0.25$ , is  $\bar{c} = 1.71$  g/l. This is nearly equal to the value determined by curve fitting.

## 5 DISCUSSION

### 5.1. Introduction

The general purpose of the experiment is to provide data on which numerical and analytical morphological models, including suspended-sediment transport, can be calibrated and verified.

Important input parameters of morphological models are:

- The percentage of suspended-sediment transport
- The shape of the equilibrium concentration-profile
- The transport formula

These subjects are discussed in sections 5.2, 5.3, 5.4 and 5.5. Adaptation lengths of flow, bed level and concentration are calculated in sec. 5.6. The bed topography is discussed in sec. 5.7. Also a mathematical approximation of the bed topography is given. In section 5.8 the results are compared with a straight flume experiment at Delft Hydraulics.

### 5.2. The Z parameter

Curve fitting of the concentration-profile prior to bend entrance yields a Z parameter of 0.28 (sec. 4.2.2.). The Z parameter is defined by:  $Z = w_s / (\beta \kappa u_*')$ . The Z parameter is a measure of the ratio of the downward flux by the fall velocity  $w_s$  and the upward flux by turbulent diffusion. Turbulent diffusion of sediment is modelled by:

$$\nu_{tc} = \beta \nu_{tm}, \text{ with } \nu_{tm} = \text{turbulent diffusion of momentum}$$

$$\nu_{tc} = \text{turbulent diffusion of mass (sediment)}$$

It is generally accepted that the turbulent diffusion coefficient of mass is greater than of momentum (Csanady 1973). Consequently  $\beta > 1$ . In the experiment, upstream of the bend entrance the bed shear velocity is equal to  $u_*' = 0.042$  m/s while the fall velocity of the suspended-sediment is:  $w_s = 0.0081$  m/s (from the supply container). This yields  $\beta \approx 1.7$

Based on a large data-set van Rijn (1984b) has calculated  $\beta$  by fitting the data with concentration verticals which are based on a parabolical-constant profile for the turbulent diffusion coefficient  $\nu_{tc}$ . (The present curve fitting is based on a parabolical profile for  $\nu_{tc}$ ). For  $w_s/u_* = 0.0081/0.042 = 0.2$  van Rijn reports effective  $\beta$  values in the range of 0.7 ... 1.8 for the experiments of Coleman (1970).

Hinze (1959) reports values of the turbulent Prandtl number  $Pr_{turb} = 1/\beta$  of 0.65 to 0.72 ( $\beta=1.4$  to 1.5) for various measurements on the distribution of heat and matter in pipe flow and two-dimensional channels.

### 5.3. Percentage of suspended-sediment transport

The percentage of suspended-sediment transport upstream of the bend is an important physical parameter of the experiment.

The division between bed and suspended load transport is somewhat arbitrary and is effected by the choice of reference level. The amount of suspended-sediment transport per unit width is defined by:

$$S_{s \text{ sus}} = \int_{z_r}^{z_s} u c dz \quad (5.1)$$

If curve fitting of the concentration-profile is performed the integral of eq.(5.1) can be computed on basis of the integral of the mathematical functions by which the measurements are approximated.

The suspended-sediment transport rate per unit width is equal to:

$$S_{s \text{ sus}} = \bar{u} \bar{c} \int_{z_r}^{z_s} r_u r_c dz = (a_0 - z_r) \bar{u} \bar{c} \int_0^1 r_u r_c d\zeta = (a_0 - z_r) \bar{u} \bar{c} \alpha_s \quad (5.2)$$

with:  $r_u, r_c$  shape functions of velocity and concentration

Suspended-sediment transport can also be estimated by averaging the measured concentrations in the vertical. The suspended-sediment transport per unit width is then approximated by:

$$S_{s \text{ sus}} \approx \frac{1}{z_s - z_r} \int_{z_r}^{z_s} u dz \int_{z_r}^{z_s} c dz \approx (z_s - z_r) \bar{u} \bar{c} \quad (5.4)$$

The depth-averaged concentration  $\bar{c}$  is computed by the method outlined in subsection 4.2.3.

The objective is to calculate the percentage of suspended-sediment transport. The total transport rate per unit width is equal to:

$$S_{\text{tot}} = a_0 \bar{u} \bar{c}_{\text{tr}} \quad (5.4)$$

in which:  $\bar{c}_{\text{tr}}$  = the transport concentration defined by eq. (5.4)

The resulting percentage of suspended-sediment transport is given in table 5.1.

Table 5.1 Percentage of suspended-sediment

method	$z_r/a_0$	$\bar{c}$ [g/l]	$S_s$	$S_s/S_{\text{tot}}$ [%]	remark
curve fitting	0.25	1.70		78 %	Z=0.28, $\alpha_s=1$
summation	0.25	1.71		78 %	

It is concluded that the percentage of suspended-sediment transport is about 80 % .

#### 5.4 Transport formulae

To simulate the experiment numerically or analytically a transport formula is necessary to predict concentration and sediment transport rates. In this section the overall transport rate of the experiment is compared with some transport formulae known from literature. It is common practice to express the total sediment transport rate by the transport concentration:  $\bar{c}_{\text{tr}} = Q_s/Q_w$  ( $S_{\text{tot}} = \bar{c}_{\text{tr}} \bar{u} a_0$  [g/m/s]). The measured transport concentration is equal to:  $\bar{c}_{\text{tr}} = 1.64$  g/l.

The transport formulae of Engelund and Hansen (1967), Ackers and White (1973), Brownlie (1981) and Van Rijn (1984c) are evaluated.

These formulae are often employed outside their range of applicability, yielding reasonable results. The Ackers-White and Brownlie formulae are

based on data sets which include data of laboratory flumes with fine sediments.

The Engelund Hansen formula reads:

$$\phi = \frac{0.05}{1-\Gamma} \frac{C^2}{g} \theta^{2.5}, \quad \text{with } \theta = \frac{di}{\Delta D_{50}}, \quad \phi = \frac{S}{\sqrt{(\Delta g D^3)}}, \quad (5.6a)$$

$$\text{or: } \bar{c}_{tr} = \rho_s \frac{1}{\bar{u}_{a0}} 0.05 \sqrt{(\Delta g D_{50}^3)} \frac{C^2}{g} \theta^{2.5} \quad (5.6b)$$

The predicted transport concentration is:  $\bar{c}_{tr} = 2.04 \text{ g/l}$   
(for  $D_{50}$  the value of the supply container is used)

The Ackers White formula reads:

$$\bar{c}_{tr} = \rho_s \frac{D_{50}}{a_0} \left(\frac{\bar{u}}{u_*}\right)^n C \left(\frac{F_{gr}}{A} - 1\right)^m \quad (5.7)$$

$$\begin{aligned} \text{with: } F_{gr} &= \frac{1}{\sqrt{(\Delta g D_{50})}} u_*^n \left(\frac{\bar{u}}{\sqrt{32 \log(10a_0/D_{50})}}\right)^{1-n} = 0.58 \\ A &= 0.23/\sqrt{D_{gr}} + 0.14 = 0.254 \\ n &= 1.00 - 0.56 \log D_{gr} = 0.660 \\ m &= 9.66/D_{gr} + 1.34 = 3.73 \\ C &= 10^{(2.86 \log D_{gr} - \log^2 D_{gr} - 3.52)} = 0.00705 \\ D_{gr} &= D_{50} (\Delta g/\nu^2)^{1/3} = 0.655 \end{aligned}$$

According to White (1972) the formula is fitted to data for which no side wall correction method has been employed, i.e.  $d=a_0$ . This yields a transport concentration equal to:  $\bar{c}_{tr} = 0.69 \text{ g/l}$

The Brownlie formula reads:

$$\bar{c}_{tr} = 7115 (F_g - F_{g0})^{1.978} i^{0.6601} (r_b/D_{50})^{-0.3301} \quad [\text{mg/l}] \quad (5.8)$$

$$\begin{aligned} \text{with: } F_g &= \frac{u}{\sqrt{(\Delta g D_{50})}} \quad \text{grain Froude number} \\ F_{g0} &= 4.596 \theta_{cr}^{0.5293} i^{-0.1405} \sigma_g^{-0.1606} \quad \text{critical grain Froude number} \\ \theta_{cr} &= 0.22 Y + 0.06 (10)^{-7.7 Y} \quad \text{critical Shields number} \\ Y &= (\Delta R)^{-0.6} \\ R_g &= \sqrt{(g D_{50}^3)/\nu} \quad \text{grain Reynolds number} \\ r_b &= 0.038 \text{ [m]}, \quad \text{hydraulic radius related to the bed according to} \\ &\quad \text{Vanoni and Brooks (1957), here } a_0 \text{ is used.} \end{aligned}$$

Prediction with this formula yields:  $\bar{c}_{tr} = 0.21 \text{ g/l}$

The Van Rijn (1984c) formulae read:

$$\text{bed-load: } \bar{c}_{trb} = \rho_s 0.005 \left( \frac{u - u_{cr}}{\sqrt{(g\Delta D_{50})}} \right)^{2.4} (D_{50}/a_0)^{1.2} \quad (5.9a)$$

$$\text{suspended-load: } \bar{c}_{trs} = \rho_s 0.012 \left( \frac{u - u_{cr}}{\sqrt{(g\Delta D_{50})}} \right)^{2.4} D_{50}/a_0 d_*^{-0.6} \quad (5.9b)$$

$$\text{total load: } \bar{c}_{tr} = \bar{c}_{trb} + \bar{c}_{trs}$$

$$\text{with: } d_* = D_{50} \sqrt[3]{(\Delta g/\nu^2)}$$

$$u_{cr} = 0.19 D_{50}^{0.1} \log(12r_b/(3D_{90})) = 0.235 \text{ m/s}$$

The transport predicted with these formulae is:  $\bar{c}_{tr} = 0$ .

This is caused by:  $u - u_{cr} < 0$

Except Engelund & Hansen none of these transport formulae predicts the actual transport concentration of the experiment.

The formula of Brownlie and Ackers & White underpredicts the transport concentration respectively by a factor 0.125 and 0.5, while Engelund & Hansen overpredicts only by 25% .

Prediction of the ratio of suspended-load and total-load could be accomplished by the equations of Van Rijn eq.(5.9a,b). Due, however, to  $u_{cr} > u$  this is impossible.

Van Rijn (1984b) has calculated the ratio of suspended-load and total-load of measurements reported by Guy et.al. (1966). It is noticed that for  $u_* / w_s > 3$  more than 50% suspended-load is present. This is in accordance with the results of the experiment:  $u_* / w_s = 5.5$ ,  $S_s \text{ sus} / S_{\text{tot}} \approx 0.80$

The performance of the Engelund & Hansen formula is comparable with the straight flume experiment, Ahmed (1990), Talmon & De Graaff (1991).

### 5.5. Bed-shear stress and sediment transport

In case of a ripple or dune covered bed the bed resistance consist of bed shear stress (friction drag) and of a pressure gradient generated by the ripple or dunes (shape drag). The total drag (which actually consist of friction and shape drag) is defined by:  $\tau = \rho g a i$

The process of sediment transport is assumed to be caused mainly by the shear stress acting on the grains. The shear stress related to sediment transport is given by:  $\tau' = \mu \tau$

in which:  $\mu$  = efficiency factor

$\tau'$  = effective grain-shear stress

$\tau$  = total drag.

To initiate sediment transport the shear stress has to exceed a critical value:  $\tau_{cr}$ . In the experiment  $\mu$  is unknown.

One of the reasons of the poor performance of the transport formulae could be caused by the relatively high resistance ( $C \approx 15 \text{ m}^{0.5}/\text{s}$ ). The data on which the transport formulae have been developed generally relate to less ( $C \approx 30 \text{ m}^{0.5}/\text{s}$ ). The transport formulae implicitly, or explicitly, contain the ratio of friction and total drag. This ratio could differ under the present conditions (the relatively large bed form height is quite exceptional). Consequently the effective grain shear-stress will differ also.

In the following the sediment transport related parameters  $\mu$  and  $\theta_{cr}$  are estimated with the aid of some empirical formulae known from literature.

The transport formulae which incorporate the critical bed-shear stress are generally proportional with:

$$\left(\frac{\mu\tau - \tau_{cr}}{\tau_{cr}}\right)^b = \left(\frac{\mu\theta - \theta_{cr}}{\theta_{cr}}\right)^b = \left(\frac{1-B}{B}\right)^b \quad (5.10a)$$

or:

$$(F_g - F_{g0})^b = \left(\frac{u - u_{cr}}{\sqrt{(g\Delta D_{50})}}\right)^b = (1-\sqrt{B})^b \left(\frac{C}{\sqrt{g}} \sqrt{\theta}\right)^b \quad (5.10b)$$

$$\text{in which: } B = \frac{\tau_{cr}}{\mu\tau}, \text{ mobility parameter} \quad (5.10c)$$

Three methods are used to estimate B. The methods are:

- 1)- The set of transport formulae by Van Rijn (1984c), eq.(5.9a,b), is used to relate the total transport concentration  $c_{tr}$  and the B parameter. Substitution of the calculated  $c_{tr}$  value yields B.
- 2)- The bed-load transport formula by Van Rijn (1984a), eq.(5.10) is used to relate the bed-load transport concentration and the B parameter. Substitution of the calculated  $c_{trb}$  value yields B.

$$c_{trb} = \frac{\rho_s}{a u} 0.053 \sqrt{(\Delta g)} \frac{D_{50}^{1.5}}{d_*^{0.3}} \left(\frac{1-B}{B}\right)^{2.1} \quad [g/l] \quad (5.11)$$

- 3)- A relation to estimate the critical Froude grain number by Brownlie (1981) is used.

$$F_{g0} = 4.596 \theta_{cr}^{0.5293} i^{-0.1405} \sigma_g^{-0.1606} \quad (5.12)$$

This relation has been obtained by Brownlie by manipulation of an empirical function which was derived to predict the flow depth.

The results are given in table 5.2. A median grain diameter of  $d_{50} = 90 \mu m$  is used. According to the Shields diagram the critical Shields number is:  $\theta_{cr} = 0.11$ .

Table 5.2 The mobility number B

	method 1	method 2	method 3
B	0.15	0.33	0.29
$\mu$ (at $\theta_{cr} = 0.11$ )	0.60	0.29	0.33
remark		80 % susp.	
		transp.	

The  $\mu$  parameter of the other 90  $\mu m$  experiments, run no. 1 to 3, is within the range:  $0.3 < \mu < 0.4$ . For run no. 4 the  $\mu$  value is within the range:  $0.25 < \mu < 0.3$  and for run no. 5 within the range  $0.25 < \mu < 0.5$ . The van Rijn (1984a) model for  $\mu$ , which is applied in the Van Rijn transport formulae, yields a distinct result:  $\mu = (C/C')^2 = (15/60)^2 =$

0.06. These results indicate that the estimate of  $\mu$ , implicitly or explicitly contained in the transport formulae, could be erroneous. The estimated value of  $\mu$  indicates that about 30...60% of the total drag is available for sediment transport.

### 5.6 Adaptation lengths

In order to formulate mathematically the interaction of flow and sediment adaptation lengths of flow velocity, bed level and concentration have been defined: Struiksmā et.al. (1986) and Olesen (1987). These adaptation lengths are defined as follows:

$$\text{adaptation length of flow: } \lambda_w = \frac{C^2}{2g} a_0 \quad (5.13a)$$

$$\text{adaptation length of bed level: } \lambda_s = \frac{1}{\pi^2} \left( \frac{W}{a_0} \right)^2 \frac{1}{G} a \quad (5.13b)$$

$$\text{adaptation length of concentration: } \lambda_c \approx a \bar{u} / w_s \quad (5.13c)$$

in which:  $G$  = coefficient of the gravitational term in the bed-load sediment direction model

The adaptation lengths for flow and bed level in the experiment are:

$$\lambda_w = 0.43 \text{ m}$$

$$\lambda_s = 0.60 \text{ m (for } G=1.1)$$

The adaptation length of concentration depends mainly on the choice of boundary condition for the concentration at reference level (Talmon, 1989). The adaptation length depends further on the value of the  $Z$  parameter, the reference height and the Chézy value. The adaptation lengths are calculated based on the assumption of a logarithmic velocity profile and a Rouse distribution for the concentration.

For  $z_r/a=0.25$ ,  $Z=0.3$  and  $C=15 \text{ m}^{1/2}/\text{s}$  the adaptation length of the concentration is:

$$\text{In case of the concentration condition: } \lambda_c = 0.26 \text{ m}$$

$$\text{In case of the gradient condition: } \lambda_c = 1.0 \text{ m}$$

### 5.7 Bed topography

The stationary bed-topography in the 180 degree bend is depicted in fig. 5. A maximum of the transverse bed slope occurs at cross sections 12...19. At this location a point-bar is present in the inner part of the bend. Overdeepening occurs at the same location in the outer part of the bend. In cross-section 41...45 again a second maximum of the transverse slope occurs.

The bed topography is approximated by a damped harmonic wave in longitudinal direction and a linear shape in transverse direction superpositioned on an axi-symmetric solution. The latter is also approximated by a linear shape. This yields the following equation:

$$a = (a_0 - \Delta b \frac{n}{\frac{1}{2}W}) e^{iks} + \Delta b_a \frac{n}{\frac{1}{2}W} \quad (5.14)$$

with:  $\Delta b$  = amplitude harmonic solution

$\Delta b_a$  = amplitude axi-symmetric solution

$s$  = coordinate in streamwise direction ( $s=0$  at point-bar)

$n$  = coordinate in transverse direction ( $n=0$  at centre-line)

$k$  = complex wave number

The last term of eq.(5.14) yields the axi-symmetric bed topography. Fitting equation (5.14) to the measured bed topography (cross section 11...46) yields:

$$\text{re}(k) = 0.72 = \frac{2\pi}{8.7}, \quad \text{im}(k) \approx 0.12, \quad \Delta b = 1.6 \text{ cm}, \quad \Delta b_a = 1.25 \text{ cm}$$

The damping  $\text{im}(k)$  is difficult to assess, consequently the accuracy is limited. These results indicate a wave length of oscillation of 8.7 m, and 63% damping ( $e^{-1}$ ) at  $s = 8$  m.

### 5.8 Comparison with a straight flume experiment at Delft Hydraulics.

The choice of parameter values of the experiment has been guided by the parameters of the straight flume experiment at Delft Hydraulics.

The bed topography of that experiment is undamped, whereas in the present bend experiment damping is noticed.

The main parameters affecting the response of the system are  $\lambda_w$ ,  $\lambda_s$  and  $\lambda_c$ . The response in terms of wavelength and damping is independent of the type of forcing. This means that the response to blocking the entrance of a straight channel, as in the case in the Delft Hydraulics experiment, or a sudden change from a straight to a curved channel, is the same.

Olesen(1987) has proposed a conceptual analytical model to determine wavelength and damping of a system with suspended-sediment transport. The dimensionless groups  $\lambda_s/\lambda_w$  and  $\lambda_c/\lambda_w$  determine the response of the system. Their values for both experiments, in case of the gradient bed boundary condition, are given in table 5.3 .

Table 5.3 Interaction parameters of the analytical model

	run6	Delft Hydraulics
$\lambda_s/\lambda_w$	1.4	0.7
$\lambda_c/\lambda_w$	2.0	1.2

It has not been succeeded to keep the  $\lambda_s/\lambda_w$  ratio the same. In the design of the experiment it was assumed that the friction coefficient would be the same for both experiments because the geometries were nearly the same. The width/depth ratio has been kept the same. Smaller  $\lambda_s/\lambda_w$  yields more damping according to Olesen's analytical theory.

## 6 CONCLUSIONS

The bed topography and sediment concentrations have been measured in a 180 degree curved flume. The median diameter of the sediment is 90  $\mu\text{m}$ .

The main features of the experiment are:

- The stationary part of the bed topography, which is forced by the curvature, is characterized by a below critical response of the transverse bed slope. Downstream of the bend entrance overdeepening occurs, this is repeated further downstream but with a smaller amplitude, at these locations the transverse bed slope is maximal.
- Non-stationary bars (free bars) are also present.

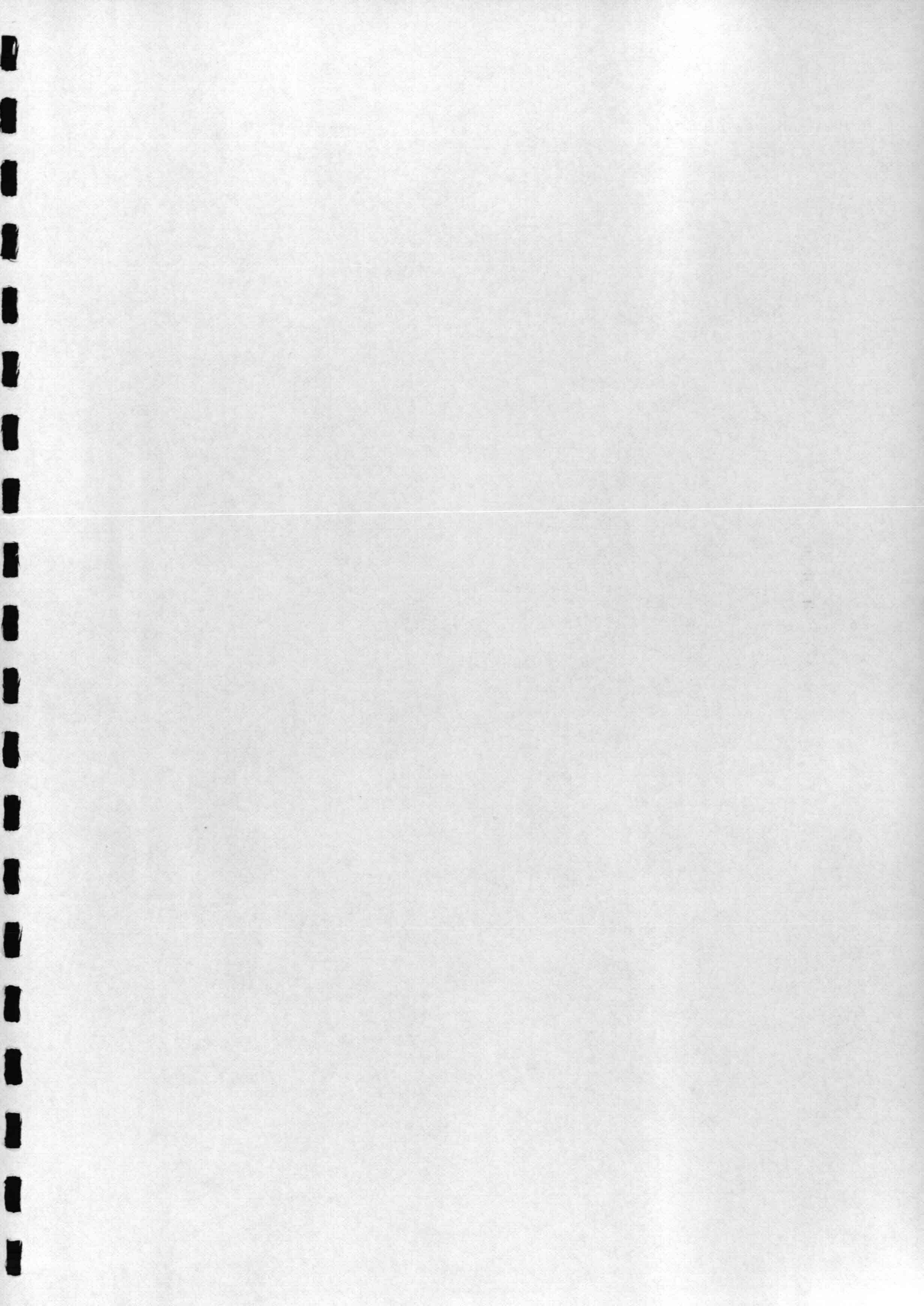
The following parameter values characterize the experiment.

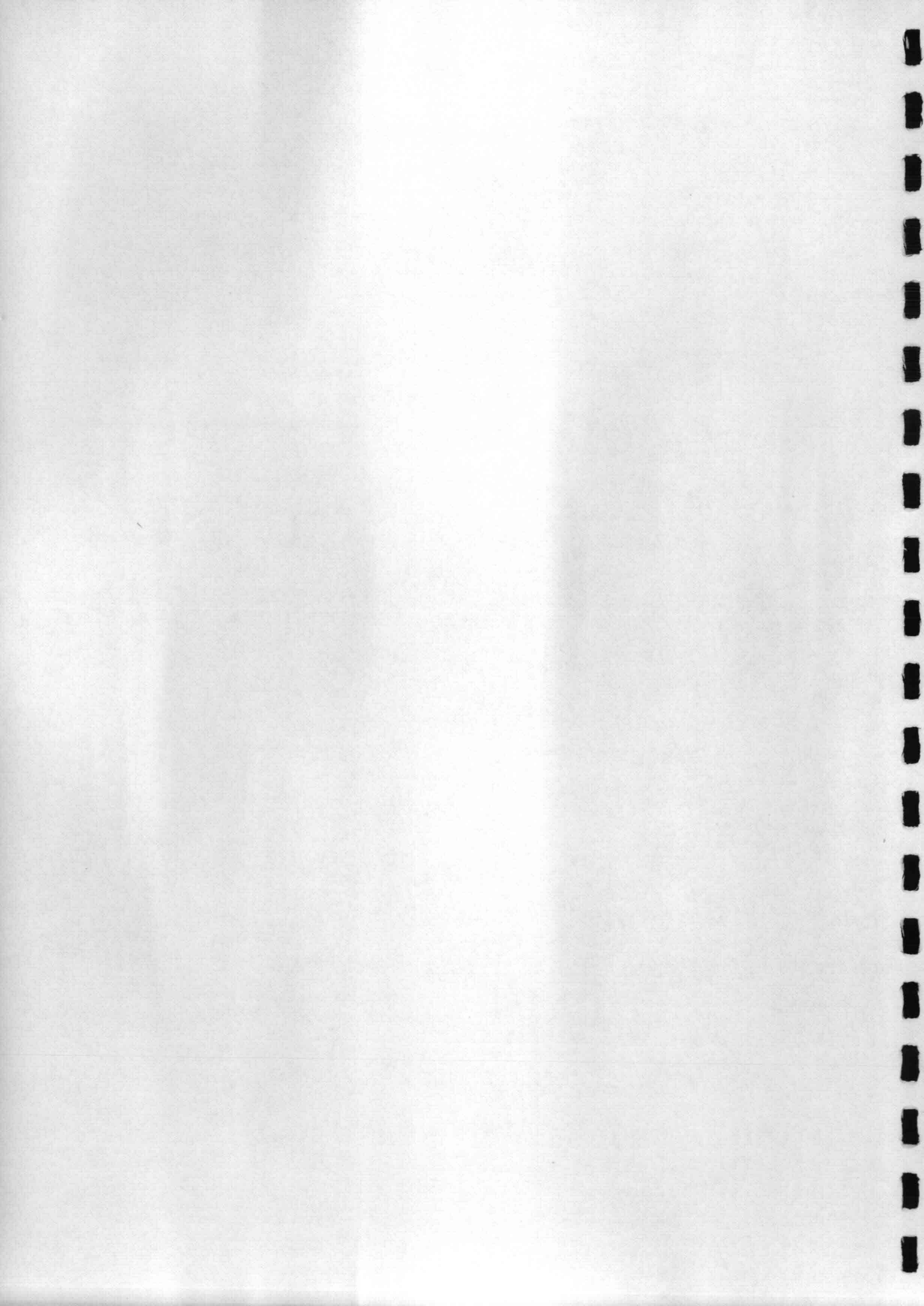
- The Chézy value is:  $C = 14.9 \text{ m}^{0.5}/\text{s}$
- With the aid of curve fitting the Z parameter of the equilibrium concentration-profile is estimated to be:  $Z = -0.28$
- Due to the exaggerated bed-form dimensions the reference height should be chosen within:  $0.2 < z_r/a < 0.3$
- The percentage suspended-sediment transport is about 80 % .

## REFERENCES

- Ackers, P. and W.R. White, 1973, Sediment transport: a new approach and analysis, *Journal of the Hydraulics Division, ASCE*, vol. 99, no. HY11, pp. 2041-2060.
- Ahmed, A.F., 1990, Hydraulic Studies on the Nile River and its Structures, Report on training in the Netherlands on River Morphology 1 Sept.-19 Okt. 1990, Delft Hydraulics, The Netherlands - Hydraulics & Sediment Research Institute Egypt.
- Brownlie, W.R., 1981, Prediction of flow depth and sediment discharge in open channels, W.M. Keck Laboratory of Hydraulics and Water Resources, California Institute Of Technology, Pasadena California, rep. no. KH-R-43A.
- Coleman, N.L., 1970, Flume studies of the sediment transfer coefficient *Water Resources*, Vol 6, no 3.
- Csanady, G.T., 1973, *Turbulent diffusion in the environment*, D. Reidel Publishing Co., Dordrecht, the Netherlands.
- Delft Hydraulics, 1986, Optical concentration meter, model OPCON, Technical manual.
- Engelund, F. and E. Hansen, 1967, A monograph on sediment transport in alluvial streams, Teknisk Forlag, Copenhagen, Denmark, pp. 62.
- Guy, H.P., D.B. Simons and E.V. Richardson, 1966, Summary of alluvial channel data from flume experiments, 1956-1961, Geological Survey Professional Paper 462-I, Washington, D.C. pp. 93.
- Olesen, K.W., Bed topography in shallow river bends  
 Doctoral thesis Delft University of Technology, 1987  
 (also: ISSN 0169-6548 *Communications on Hydraulic and Geotechnical Engineering*, Delft University of Technology, Faculty of Civil Engineering).
- Rijn, L.C. van, 1984a, Sediment transport, part I: bed load transport, *Journal of Hydraulic Engineering*, Vol 110, no. 10, pp. 1431-1456.
- Rijn, L.C. van, 1984b, Sediment transport, part II: suspended load transport, *Journal of Hydraulic Engineering*, Vol 110, no. 11, pp. 1613-1641.
- Rijn, L.C. van, 1984c, Sediment transport, part III: bed form and alluvial roughness, *Journal of Hydraulic Engineering*, Vol 110, no. 12, pp. 1733-1754.

- Rijn, L.C. van, 1987, Mathematical modelling of morphological processes in the case of suspended sediment transport  
Doctoral thesis Delft University of Technology, 1987  
(also: Delft Hydraulics Communication no. 382).
- Slot, R.E. and H.J. Geldof, 1986, An improved settling tube system for sand. ISSN 0169-6548, Communications on Hydraulics and Geotechnical Engineering, Delft University of Technology, Faculty of Civil Engineering, rep. no. 86-12.
- Struiksma, N. and A. Crosato, 1989, Analysis of a 2-DH bed topography model for rivers, in: River Meandering, A.G.U. Water resources monograph, vol. 12, Washington D.C., U.S.A.
- Struiksma, N.; K.W. Olesen, C. Flokstra and H.J. de Vriend, 1986, Bed deformation in alluvial channel bends. IAHR, Journal of Hydraulic Research, vol. 23, no. 1, pp. 57-79.
- Talmon, A.M., 1989, A theoretical model for suspended sediment transport in river bends, ISSN 0169-6548, Communications on Hydraulic and Geotechnical Engineering, Delft University of Technology, Faculty of Civil Engineering, rep. no. 89-5.
- Talmon, A.M., and J. de Graaff, 1990, A suspended-load experiment in a straight flume at Delft Hydraulics, Delft Univ. of Techn., Dep. Civil Eng., rep. no. 4-91, 1991
- Vanoni, V.A. and N.H. Brooks, 1957, Laboratory studies of the roughness and suspended load of alluvial streams, Rep. no. E-68, Publication no. 149, California Institute of Technology Pasadena, California, pp. 121.
- White, W.R., 1972, Sediment transport in channels: a general function, rep. INT 104, Hydraulics Research Station, England.





Appendix A: Ensemble averaged water depths.

In this appendix the ensemble averaged relative water depths of the 21 measurements are tabulated.

Relative mean water depth  $a/a_0$ . ( $a_0 = 0.038$  m)

from inner side of bend	CS01	CS02	CS03	CS04	CS05	CS06	CS07
0.05	1.21	1.10	1.17	1.16	1.26	1.15	1.13
0.10	1.18	1.10	1.19	1.16	1.19	1.17	1.11
0.15	1.04	1.09	1.13	1.07	1.02	1.16	1.08
0.20	1.03	0.97	0.94	0.92	1.00	1.04	0.97
0.25	1.06	0.94	0.94	0.90	0.97	0.91	0.85
0.30	0.99	0.93	1.00	0.89	0.93	0.90	0.78
0.35	0.89	0.95	0.87	0.96	0.84	0.85	0.83
0.40	0.87	0.92	0.90	0.94	0.87	0.81	0.92
0.45	0.92	0.92	0.91	0.90	0.87	0.82	0.96

from inner side of bend	CS08	CS09	CS10	CS11	CS12	CS13	CS14
0.05	1.03	0.88	0.73	0.60	0.53	0.56	0.61
0.10	1.00	0.89	0.80	0.62	0.64	0.53	0.57
0.15	1.11	0.94	0.91	0.75	0.68	0.58	0.58
0.20	1.05	0.92	0.82	0.81	0.69	0.73	0.68
0.25	0.90	0.98	0.86	0.94	0.83	0.81	0.92
0.30	0.88	0.93	0.98	1.01	0.97	0.91	1.05
0.35	0.95	1.00	1.16	1.13	1.21	1.24	1.28
0.40	1.02	1.05	1.25	1.32	1.47	1.42	1.36
0.45	1.17	1.26	1.45	1.60	1.59	1.62	1.56

from inner side of bend	CS15	CS16	CS17	CS18	CS19	CS20	CS21
0.05	0.76	0.93	1.00	0.90	0.89	0.98	1.05
0.10	0.73	0.81	0.96	0.94	0.88	0.92	0.94
0.15	0.68	0.77	0.87	1.03	0.92	0.92	0.87
0.20	0.79	0.77	0.84	0.91	0.84	0.90	0.90
0.25	0.90	0.86	0.83	0.87	0.86	0.90	0.99
0.30	0.96	1.05	0.84	0.92	0.96	1.00	0.97
0.35	1.14	1.19	1.01	1.07	1.11	1.00	1.11
0.40	1.31	1.30	1.05	1.08	1.16	1.13	1.05
0.45	1.47	1.31	1.15	1.20	1.17	1.21	1.10

from inner side of bend	CS22	CS23	CS24	CS25	CS26	CS27	CS28
0.05	1.02	0.98	1.07	0.86	0.96	0.86	0.94
0.10	0.98	0.94	0.98	0.90	0.97	0.90	0.83
0.15	1.00	0.97	1.01	0.95	0.91	0.96	0.89
0.20	0.80	0.99	0.99	1.02	0.96	1.03	0.96
0.25	0.96	1.00	0.98	0.96	1.03	0.97	1.00
0.30	1.01	1.00	0.92	0.95	1.03	0.92	1.03
0.35	0.99	1.00	1.00	1.04	1.06	1.00	1.16
0.40	1.03	1.04	1.07	1.10	1.09	1.20	1.10
0.45	1.13	1.09	1.02	1.10	1.09	1.16	1.16

from inner side of bend	CS29	CS30	CS31	CS32	CS33	CS34	CS35
0.05	0.74	0.68	0.73	0.72	0.82	0.95	0.89
0.10	0.80	0.74	0.76	0.69	0.78	0.86	0.83
0.15	0.91	0.81	0.78	0.76	0.78	0.86	0.86
0.20	0.88	0.98	0.90	0.81	0.85	0.78	0.89
0.25	0.91	0.92	0.97	1.05	1.03	0.91	0.89
0.30	1.00	1.05	1.04	1.08	1.04	1.05	0.94
0.35	1.00	1.01	1.11	1.17	1.17	1.19	1.06
0.40	1.24	1.11	1.17	1.26	1.28	1.24	1.18
0.45	1.23	1.23	1.31	1.42	1.37	1.36	1.20

from inner side of bend	CS36	CS37	CS38	CS39	CS40	CS41	CS42
0.05	0.89	0.88	0.90	0.76	0.89	0.98	0.89
0.10	0.88	0.90	0.93	0.77	0.92	0.90	0.85
0.15	0.86	0.90	0.89	0.84	0.90	0.92	0.88
0.20	0.92	1.01	0.98	0.94	0.92	0.99	1.01
0.25	0.93	0.99	0.99	0.95	1.03	0.95	1.12
0.30	0.97	1.02	0.99	1.04	1.00	0.97	1.09
0.35	1.09	1.03	1.07	1.05	1.24	1.19	1.11
0.40	1.12	1.15	1.06	1.25	1.23	1.16	1.16
0.45	1.23	1.25	1.13	1.30	1.26	1.21	1.21

from inner side of bend	CS43	CS44	CS45	CS46	CS47	CS48
0.05	0.82	0.82	0.84	0.85	1.04	1.07
0.10	0.87	0.89	0.86	0.82	0.84	0.96
0.15	0.89	0.88	0.94	0.95	0.83	0.98
0.20	0.87	0.89	0.93	1.01	0.94	0.96
0.25	0.91	1.00	0.97	1.02	0.98	0.98
0.30	0.97	1.16	1.04	1.12	1.09	1.04
0.35	1.08	1.18	1.11	1.15	1.12	1.14
0.40	1.21	1.19	1.21	1.13	1.09	1.04
0.45	1.16	1.29	1.24	1.10	1.14	1.06

Appendix B: Concentration dataCross section 1.

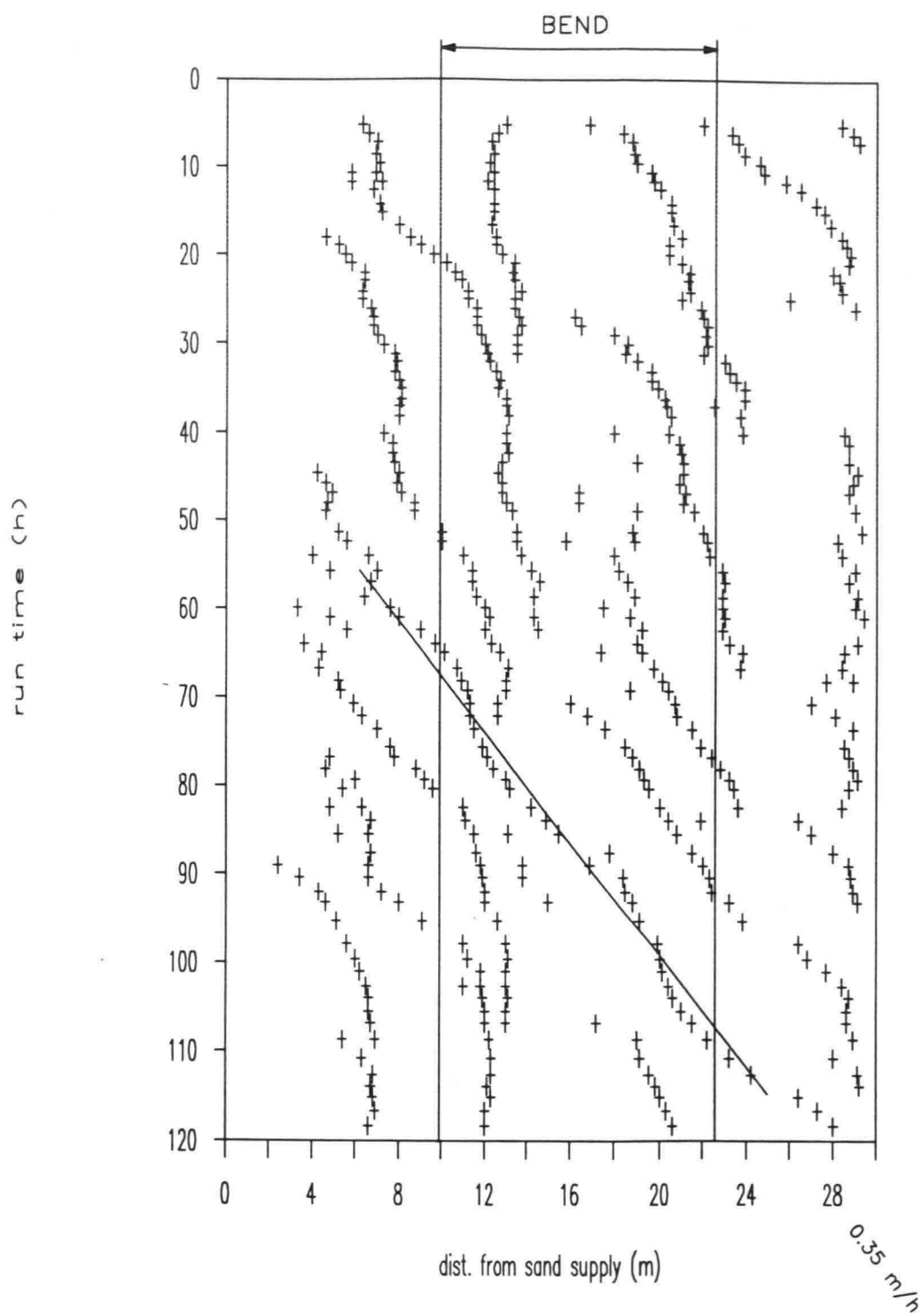
location in cross- direction	Mean water depth	Distance beneath water surface	Concen- tration					
[y/W]	[mm]	[mm]	[g/l]					
1/2	33	5	0.277	0.374	0.513	0.606		
		8	0.448					
		10	0.642	0.686	0.562	0.646	0.558	0.619
			0.588	0.583				
		13	0.954					
		15	0.718	1.243	0.921	0.652	1.395	0.616
			0.669	0.538				
		20	1.259	1.284	1.764	0.871	1.194	
25	1.236	1.307	1.487	1.978	1.884			

Appendix C: Free bars.

Free bars are observed during the whole bend experiment. Every one a two hours the positions of the bars are tracked by visual observation at side walls of the channel.

The results of these observations are given in fig. C1...C4. The positions of the top (H) and the trough (L) of the bars at the left and the right side walls are given.

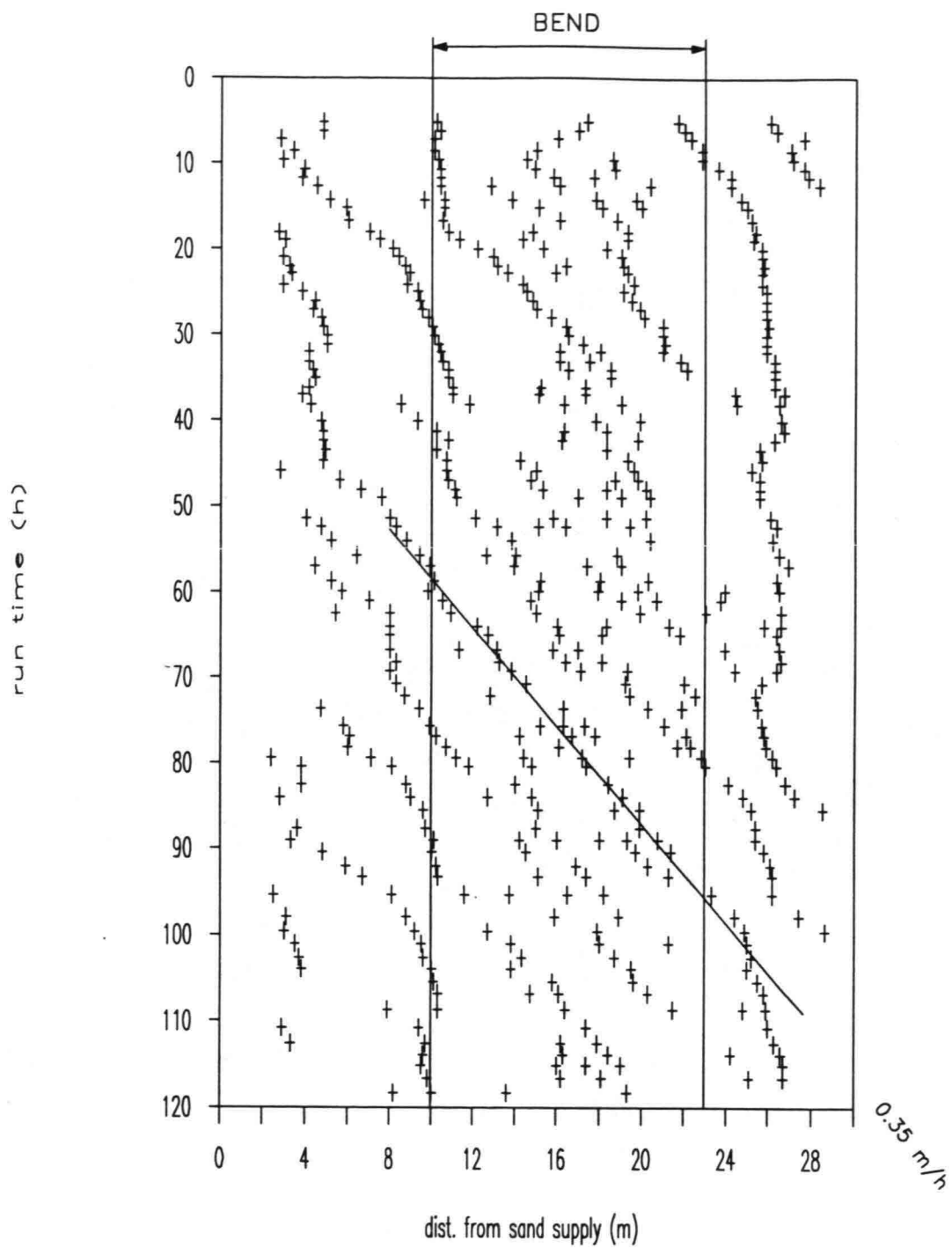
The free bar wave length is: 4.9 m, celerity 0.35 m/h.



POSITION FREE BARS CREST, INNERSIDE BEND

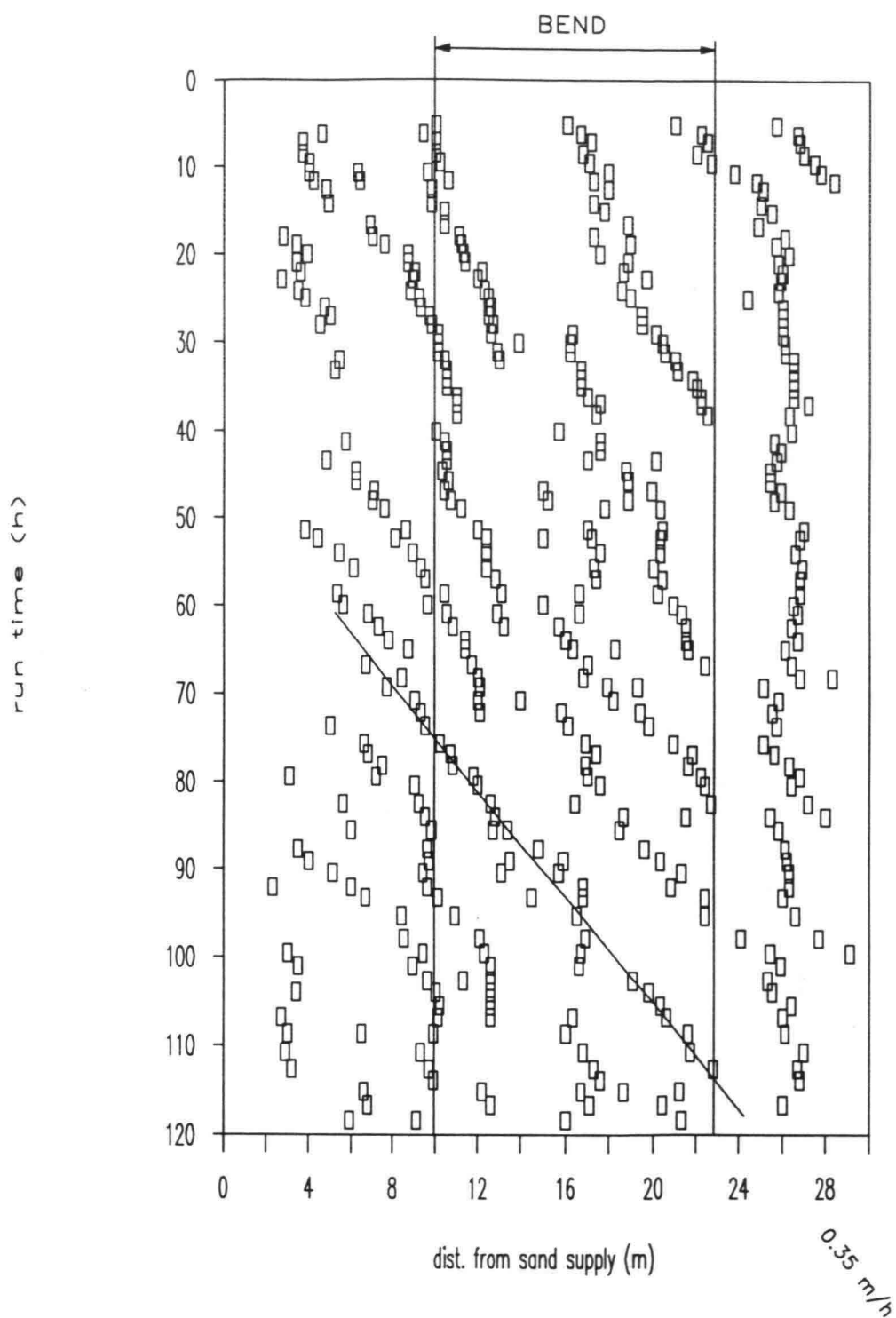
FIG. C1

DELFT UNIVERSITY OF TECHNOLOGY



POSITION BAR CREST, OUTER SIDE BEND

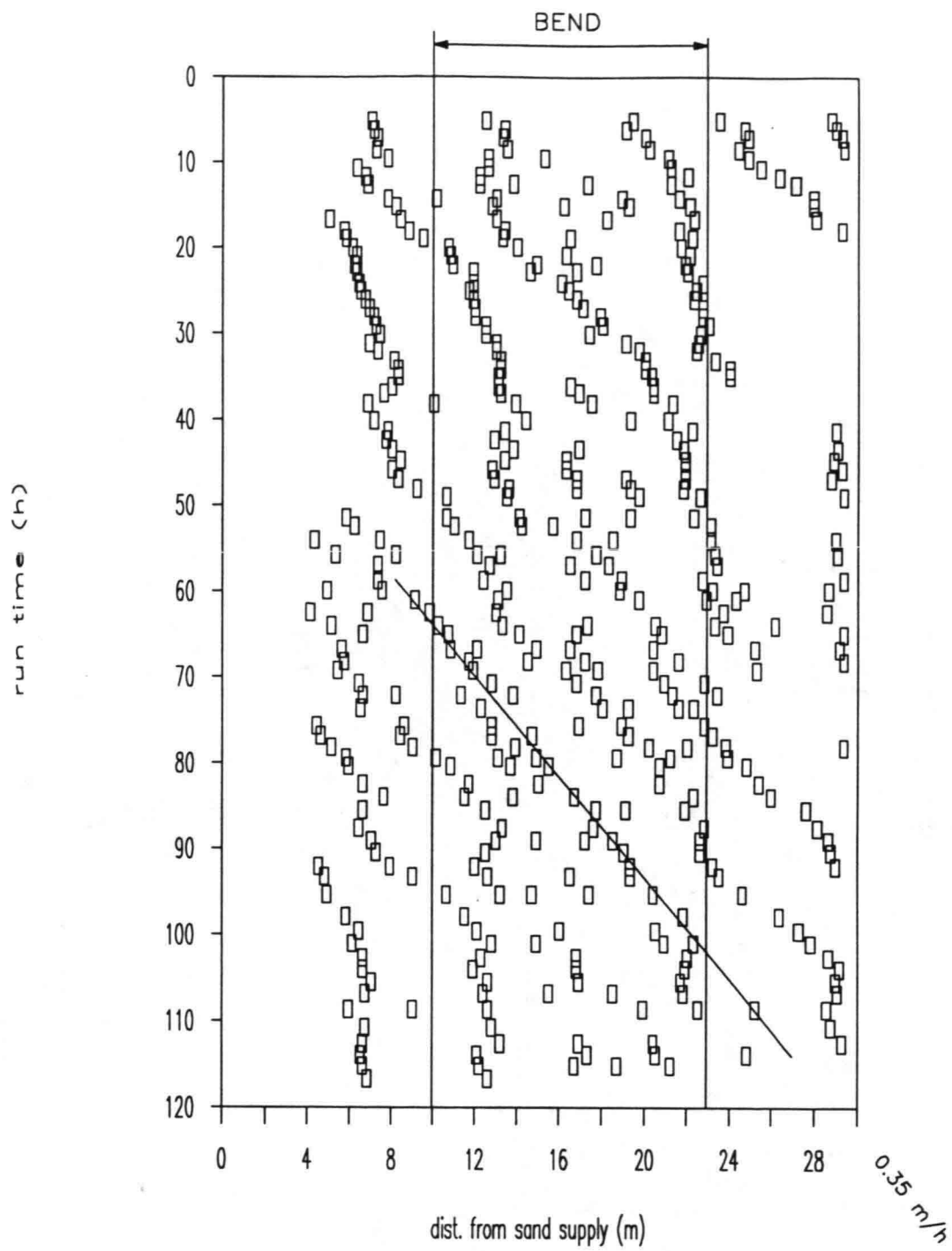
FIG. C2



POSITION BAR TROUGH, INNER SIDE BEND

FIG. C3

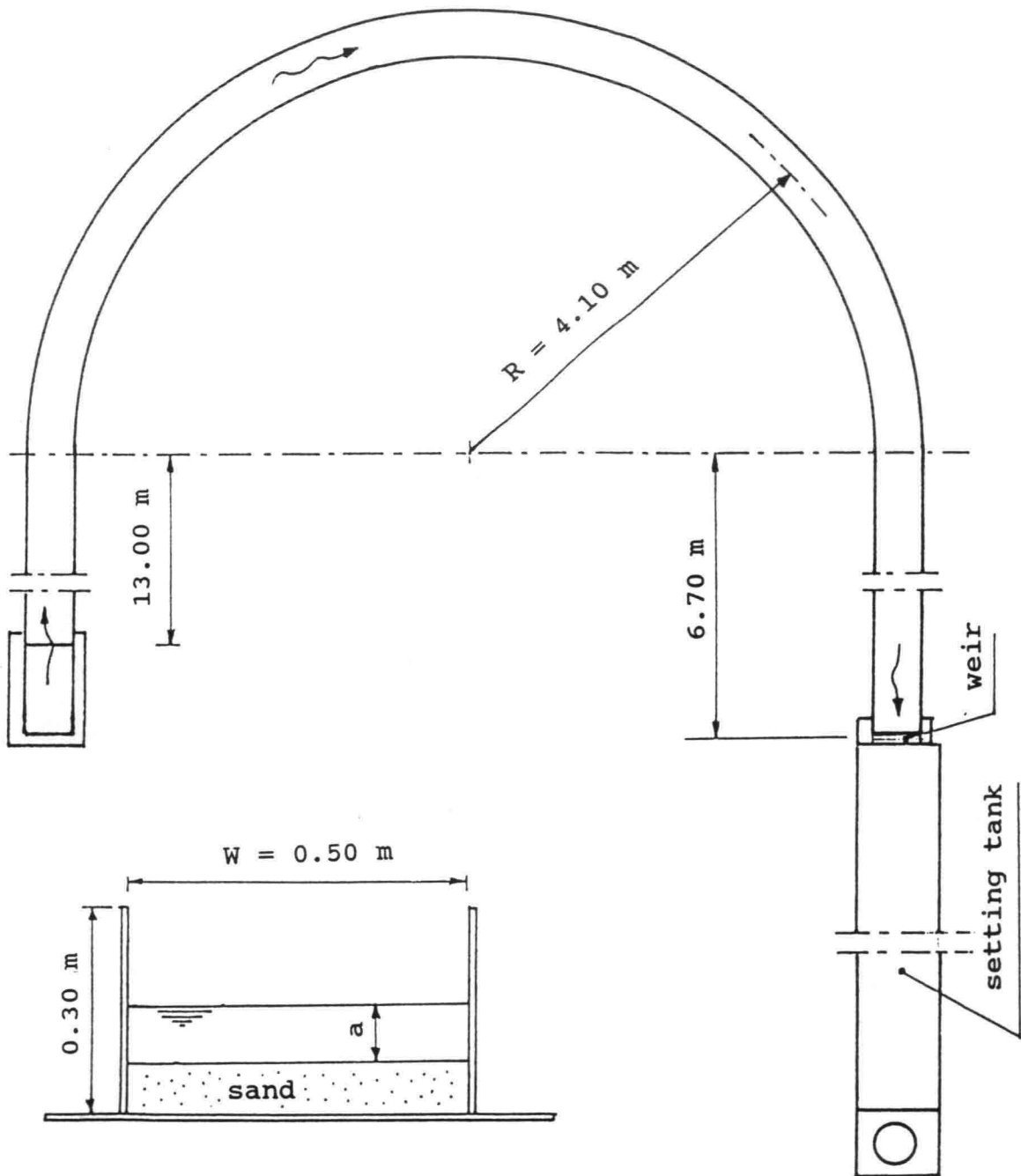
DELFT UNIVERSITY OF TECHNOLOGY



POSITION BAR TROUGH, OUTER SIDE BEND

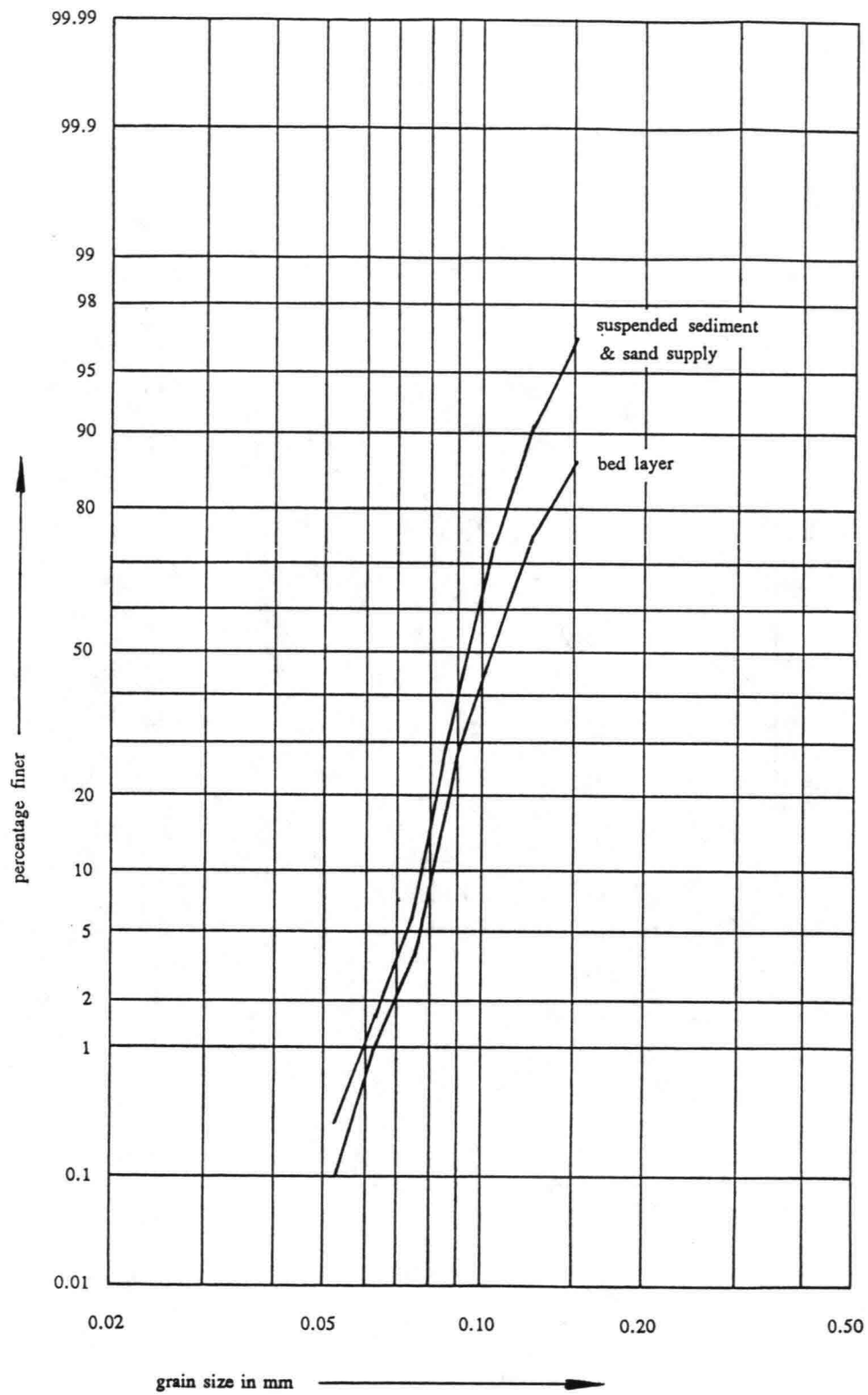
DELFT UNIVERSITY OF TECHNOLOGY

FIG. C4



LAYOUT, LFM CURVED FLUME

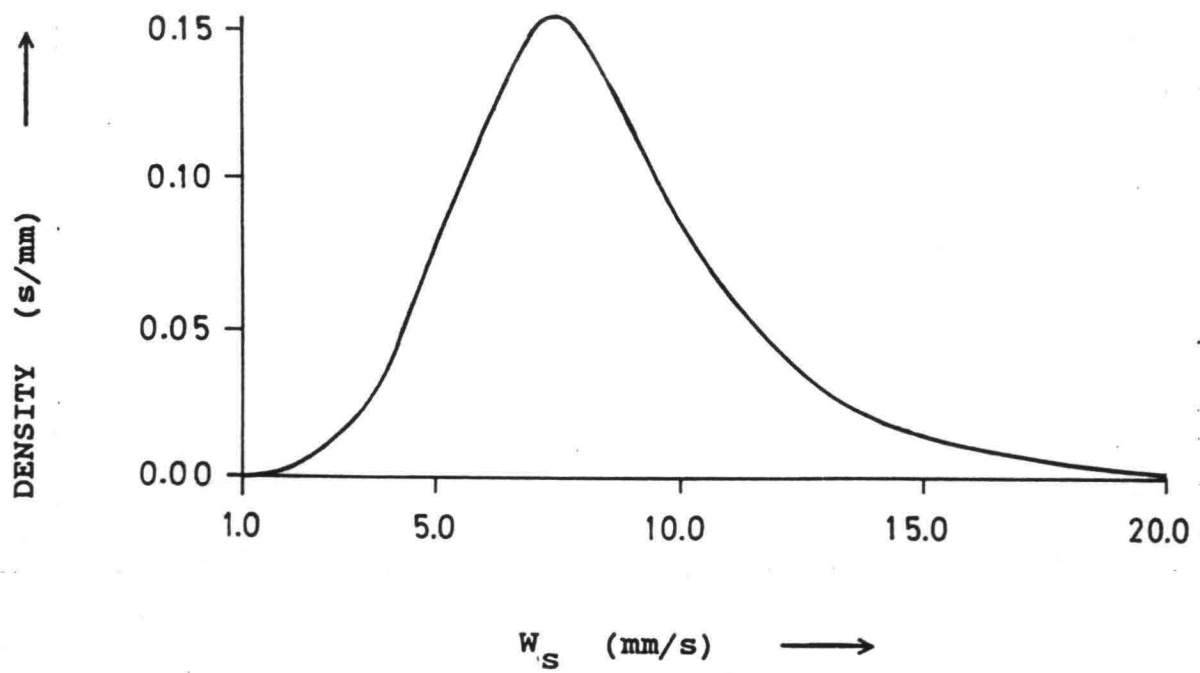
FIG. 1



SIEVE CURVES OF SEDIMENT

DELFT UNIVERSITY OF TECHNOLOGY

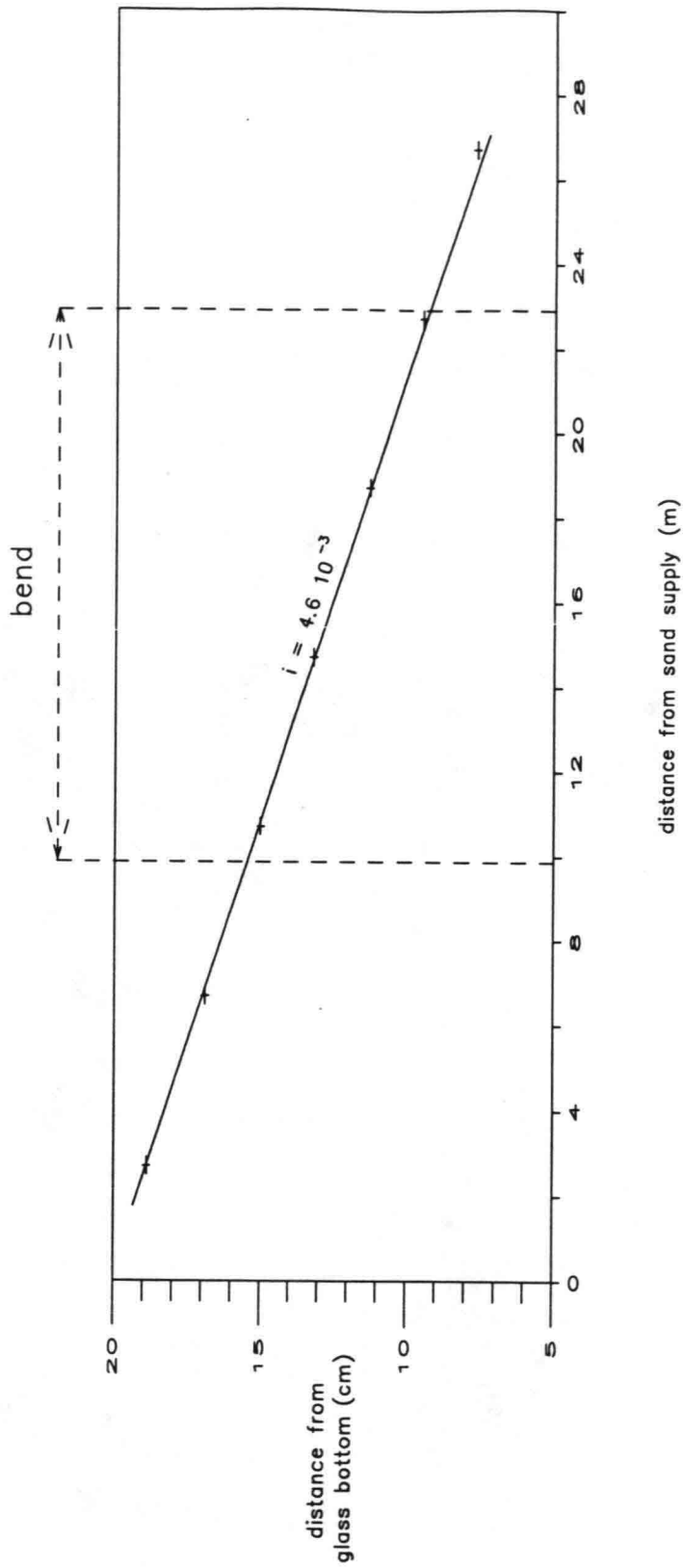
FIG. 2



PROBABILITY DENSITY DISTRIBUTION OF FALL  
VELOCITY

FIG. 3

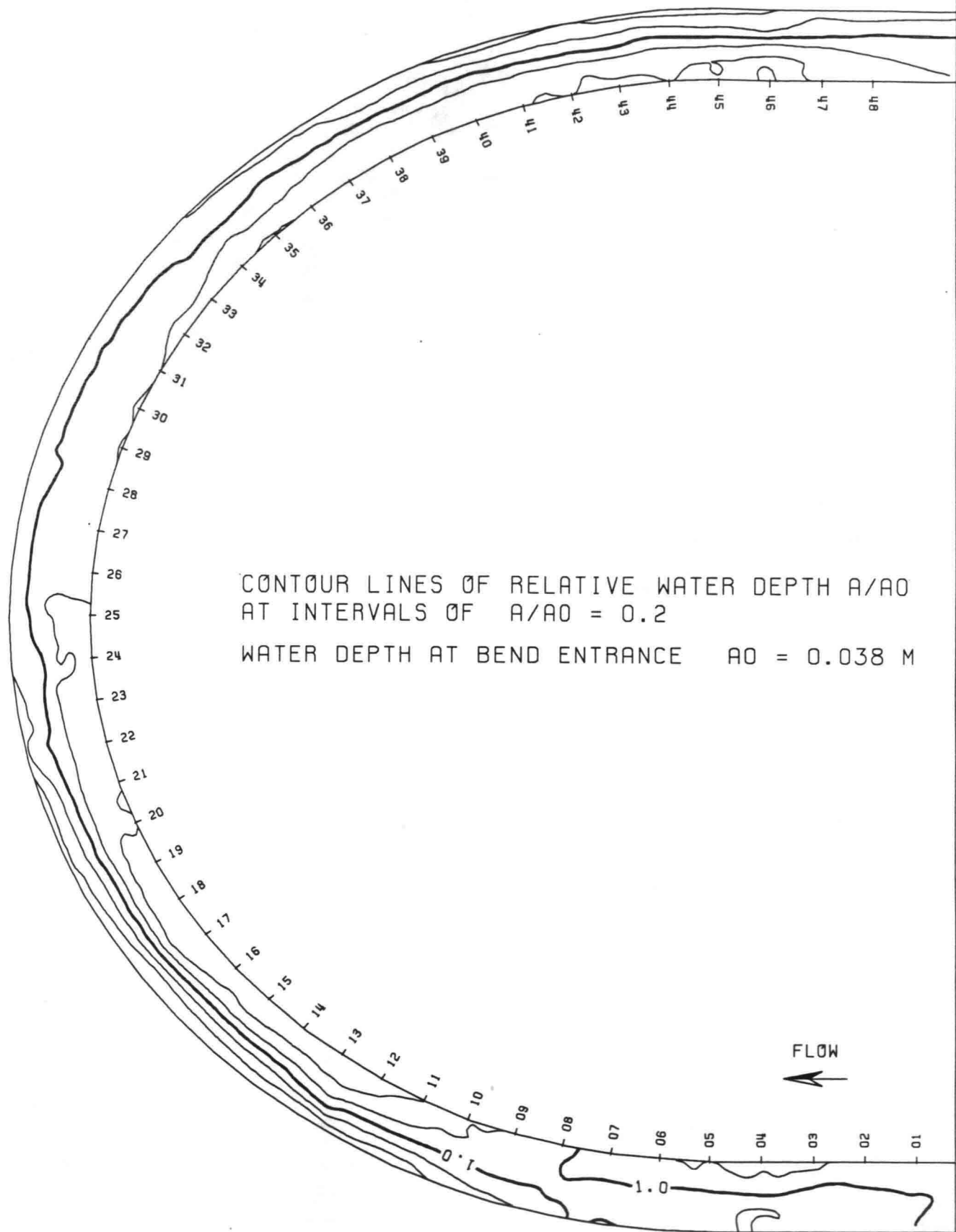
DELFT UNIVERSITY OF TECHNOLOGY



LONGITUDINAL WATER LEVEL SLOPE

DELFT UNIVERSITY OF TECHNOLOGY

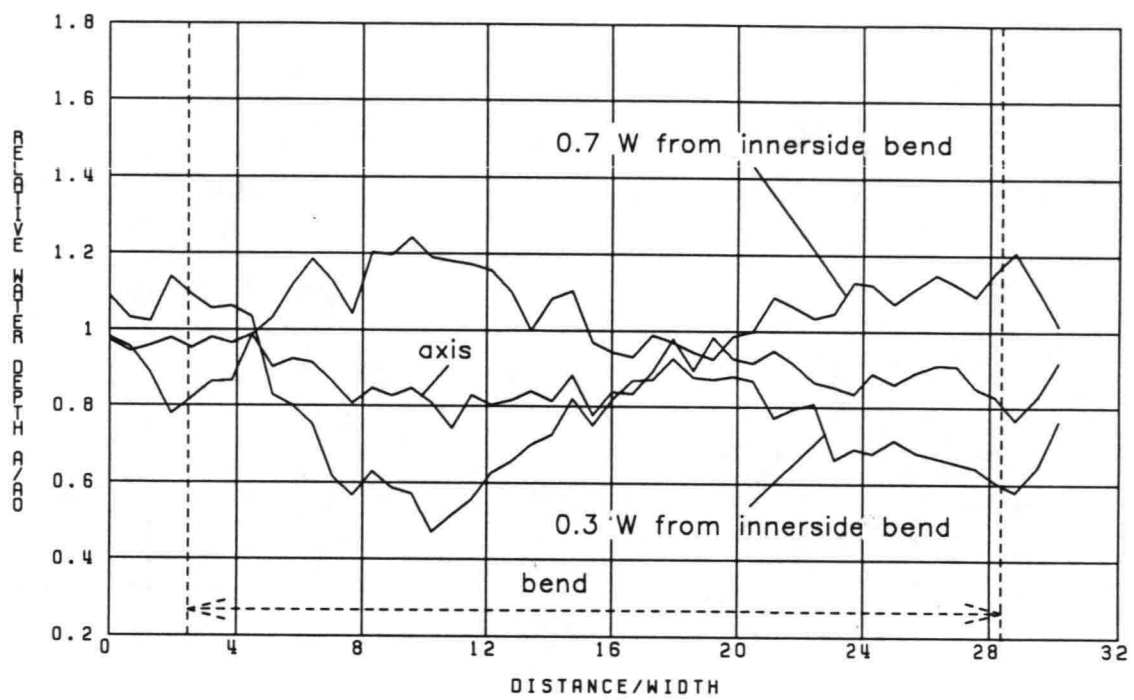
FIG. 4



MODEL OF RIVER BEND, SUSPENDED-LOAD EXPERIMENT  
 ENSEMBLE MEAN OF 23 LONGITUDINAL TRAVERSES

DELFT UNIVERSITY OF TECHNOLOGY

FIG.5

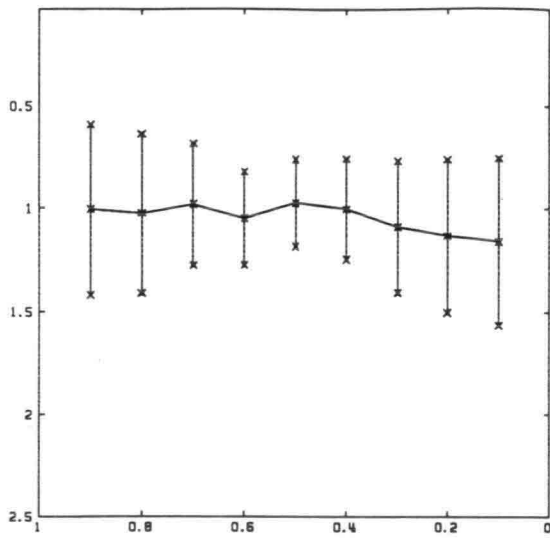


W = 0.5 M    A0 = 0.030 M

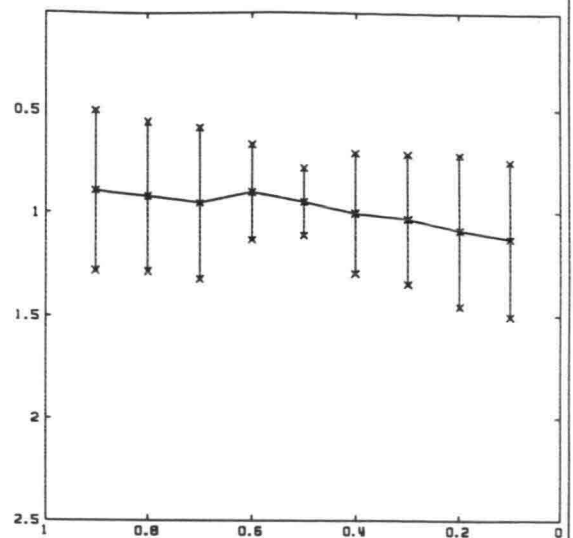
LONGITUDINAL PROFILE OF THE WATER DEPTH

FIG 6

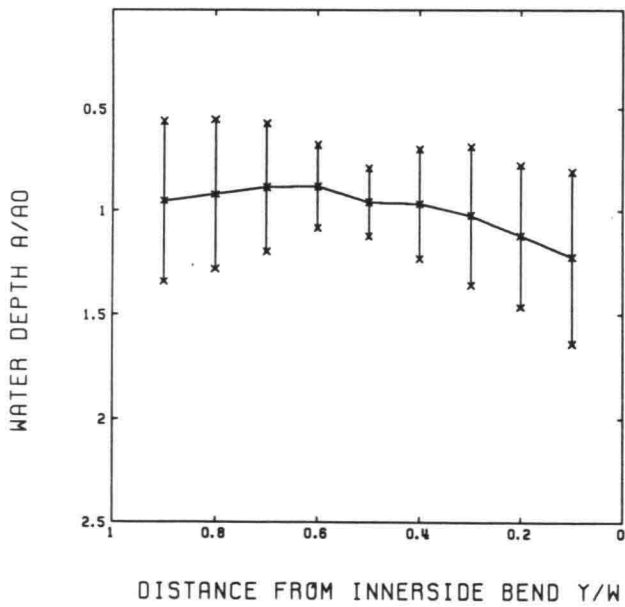
DELFT UNIVERSITY OF TECHNOLOGY



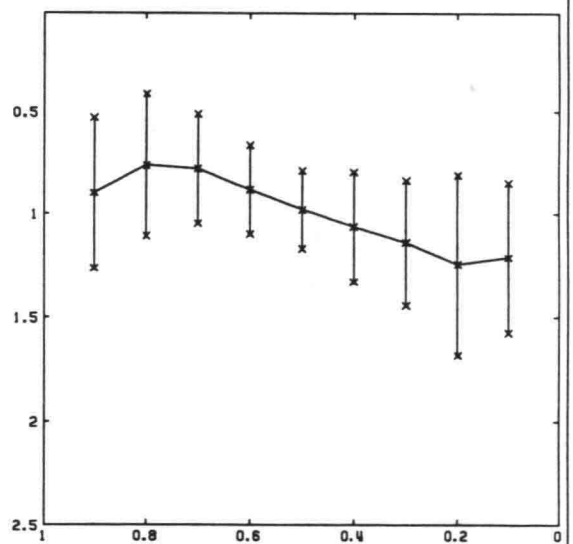
CROSS-SECTION 1



CROSS-SECTION 2



CROSS-SECTION 3



CROSS-SECTION 4

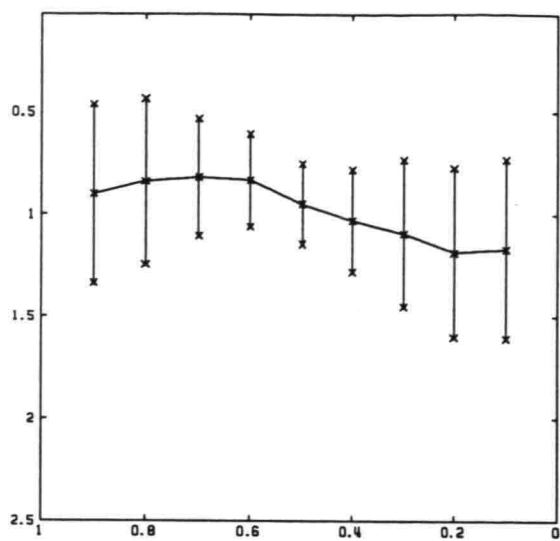
$W = 0.5 \text{ M}$      $AO = 0.038 \text{ M}$

$\bar{x} \pm \sigma$  OF 23 MEASUREMENTS

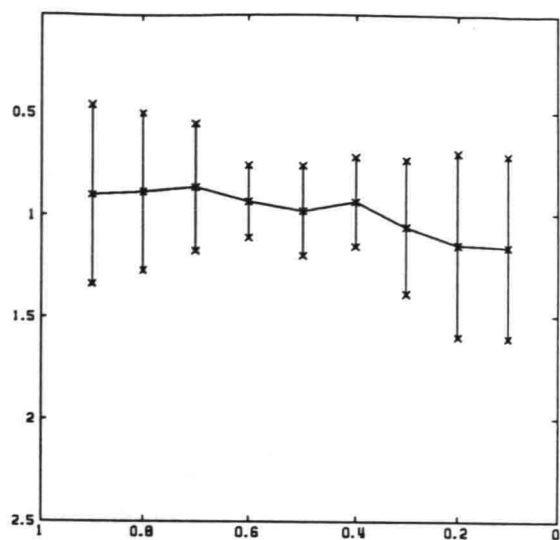
WATER DEPTH IN CROSS-DIRECTION

FIG 7A

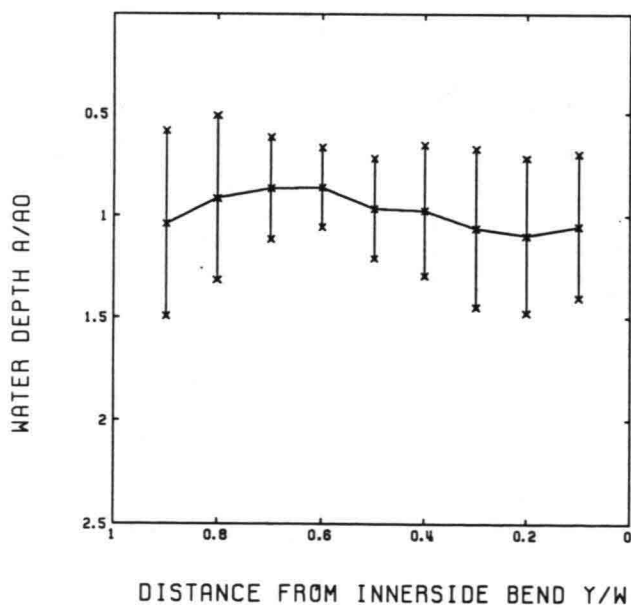
DELFT UNIVERSITY OF TECHNOLOGY



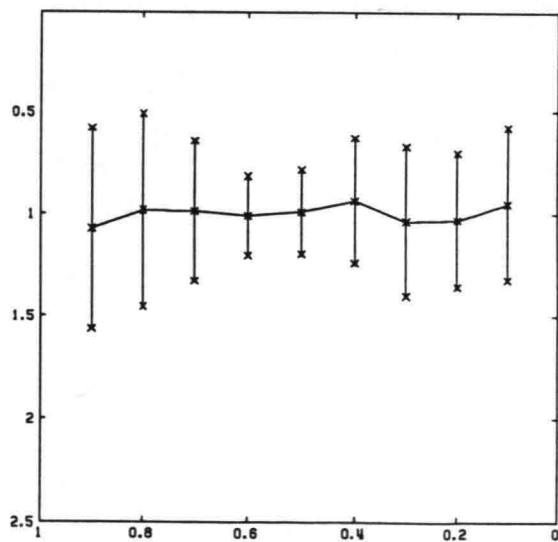
CROSS-SECTION 5



CROSS-SECTION 6



CROSS-SECTION 7



CROSS-SECTION 8

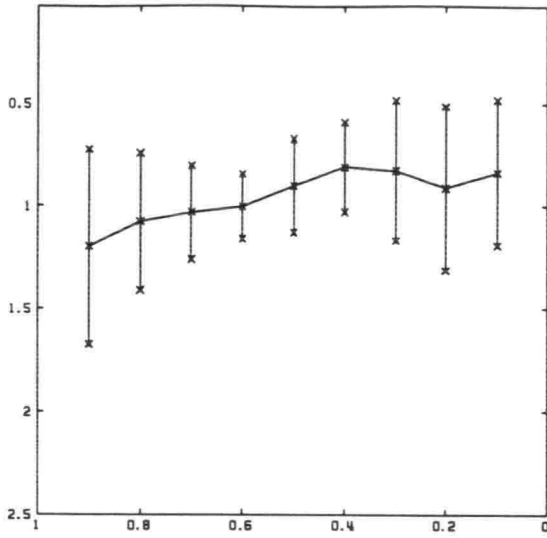
W = 0.5 M    AO = 0.030 M

$\bar{x} \pm \sigma$  OF 23 MEASUREMENTS

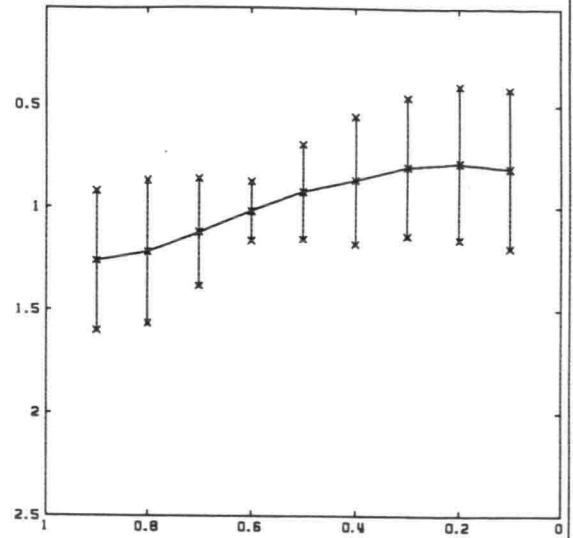
WATER DEPTH IN CROSS-DIRECTION

FIG 7B

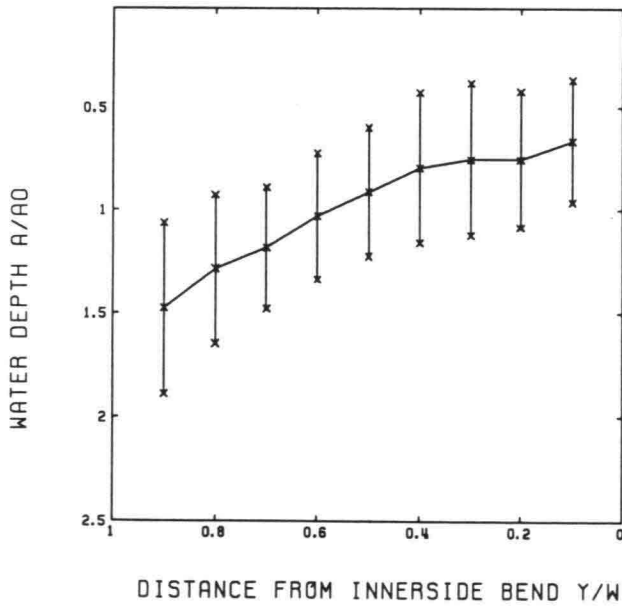
DELFT UNIVERSITY OF TECHNOLOGY



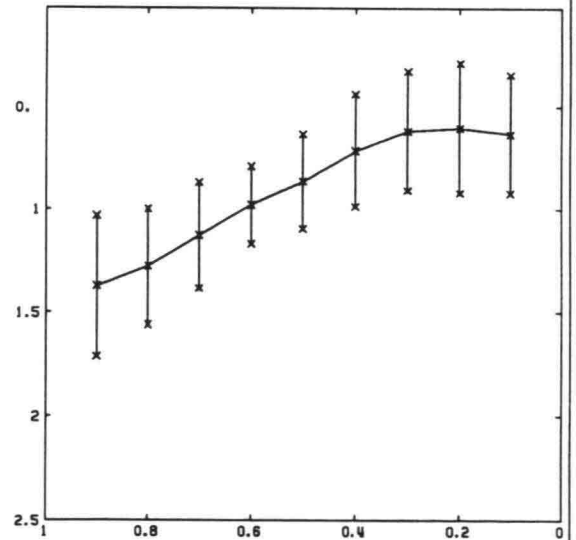
CROSS-SECTION 9



CROSS-SECTION 10



CROSS-SECTION 11



CROSS-SECTION 12

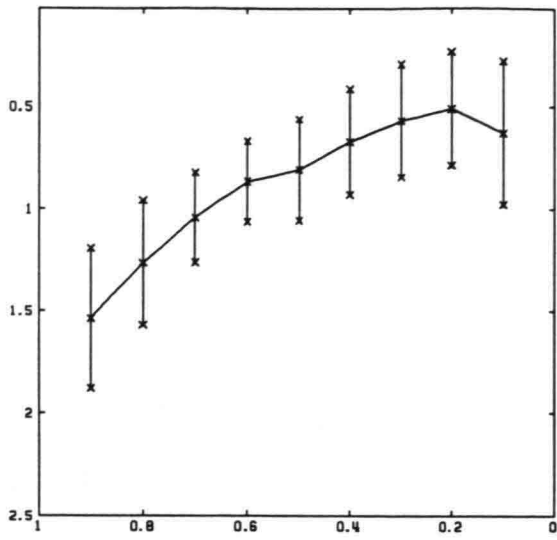
W = 0.5 M    AO = 0.038 M

$\bar{x} \pm \sigma$  OF 23 MEASUREMENTS

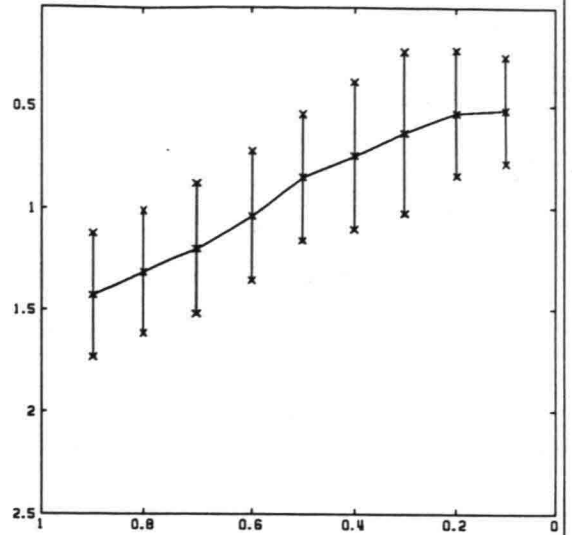
WATER DEPTH IN CROSS-DIRECTION

FIG 7C

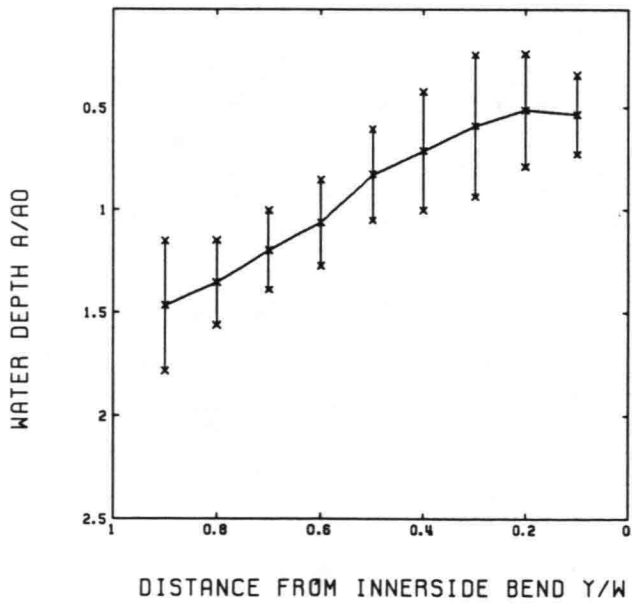
DELFT UNIVERSITY OF TECHNOLOGY



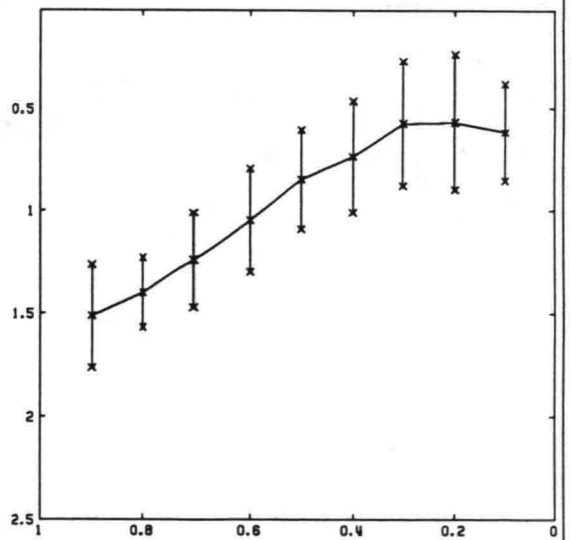
CROSS-SECTION 13



CROSS-SECTION 14



CROSS-SECTION 15



CROSS-SECTION 16

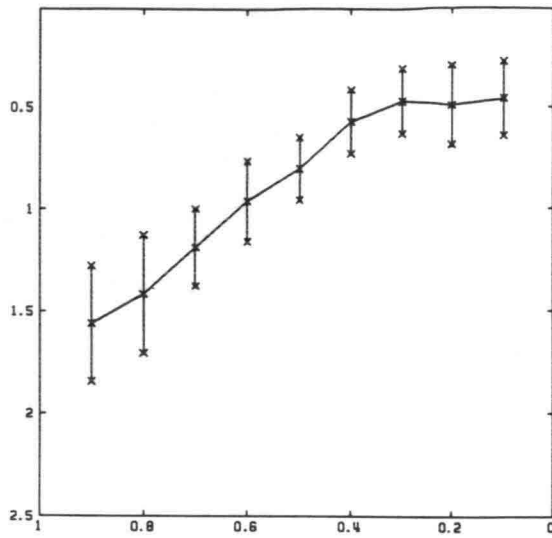
$W = 0.5 \text{ M}$      $AO = 0.030 \text{ M}$

$\bar{y} \pm \sigma$  OF 23 MEASUREMENTS

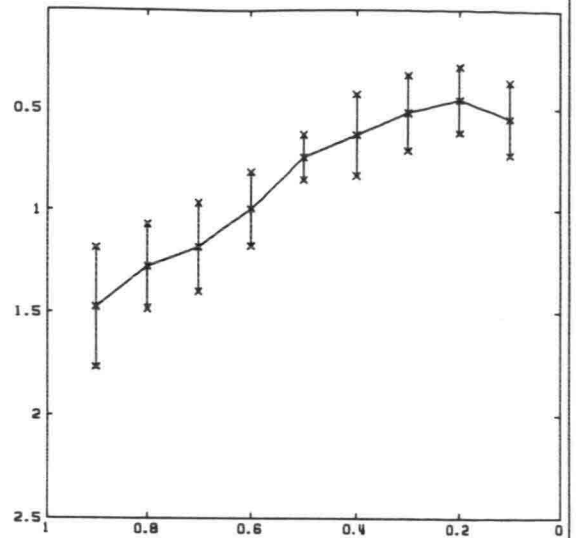
WATER DEPTH IN CROSS-DIRECTION

FIG 7D

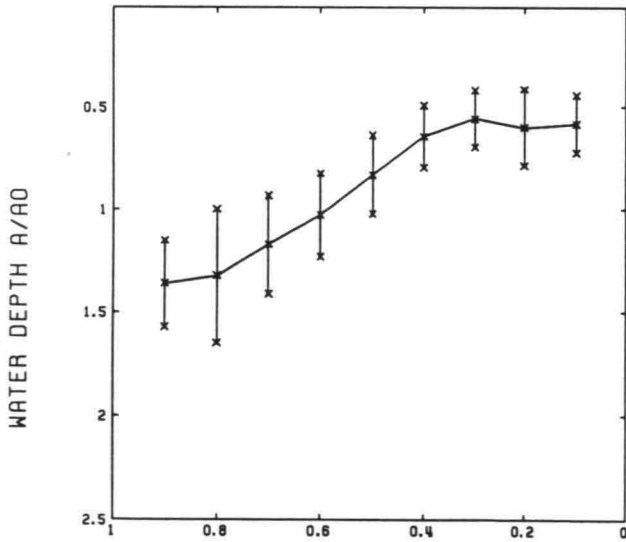
DELFT UNIVERSITY OF TECHNOLOGY



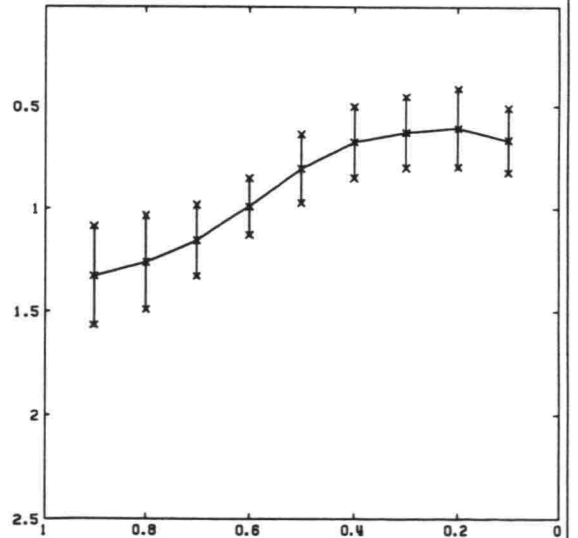
CROSS-SECTION 17



CROSS-SECTION 18



CROSS-SECTION 19



CROSS-SECTION 20

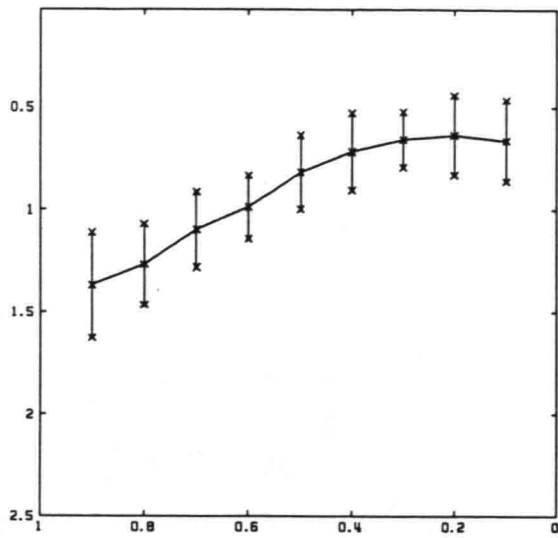
$W = 0.5 \text{ M}$      $AO = 0.038 \text{ M}$

$\bar{x} \pm \sigma$  OF 23 MEASUREMENTS

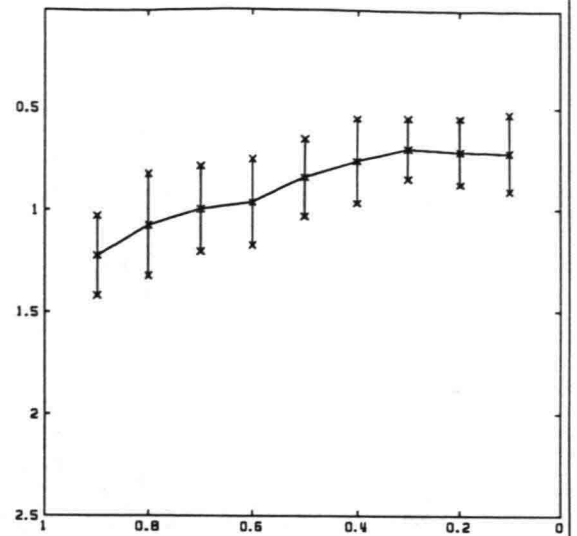
WATER DEPTH IN CROSS-DIRECTION

FIG 7E

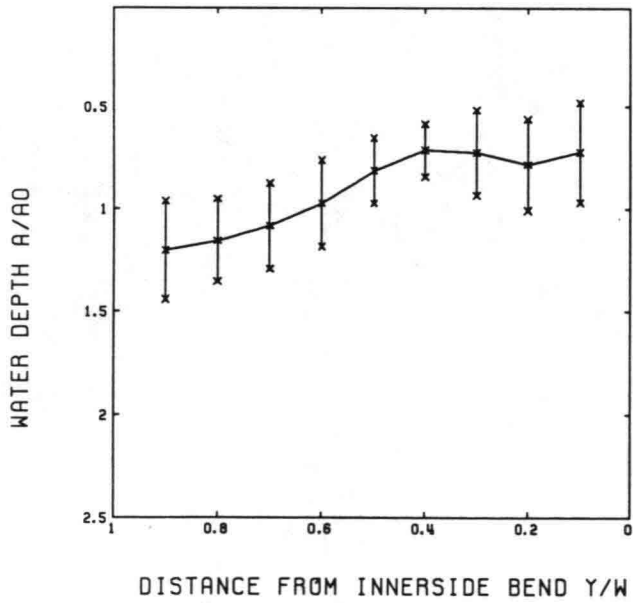
DELFT UNIVERSITY OF TECHNOLOGY



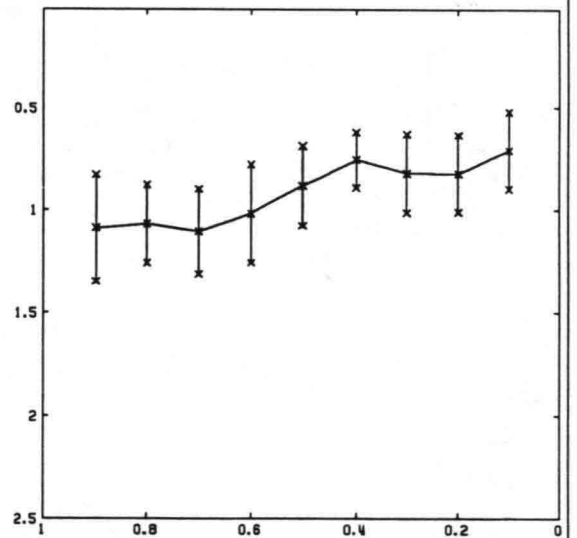
CROSS-SECTION 21



CROSS-SECTION 22



CROSS-SECTION 23



CROSS-SECTION 24

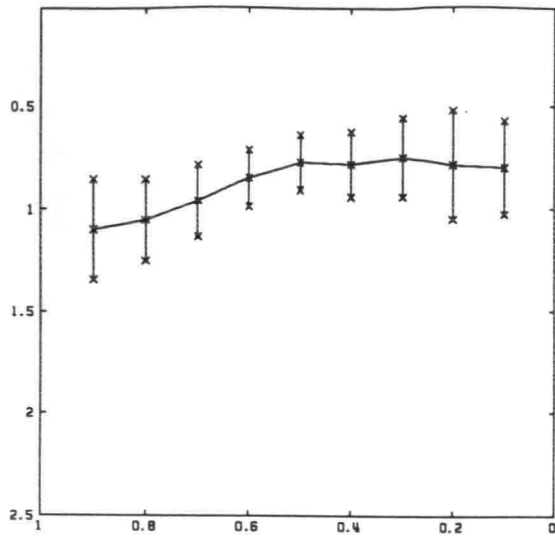
W = 0.5 M    AO = 0.038 M

$\bar{x} \pm \sigma$  OF 23 MEASUREMENTS

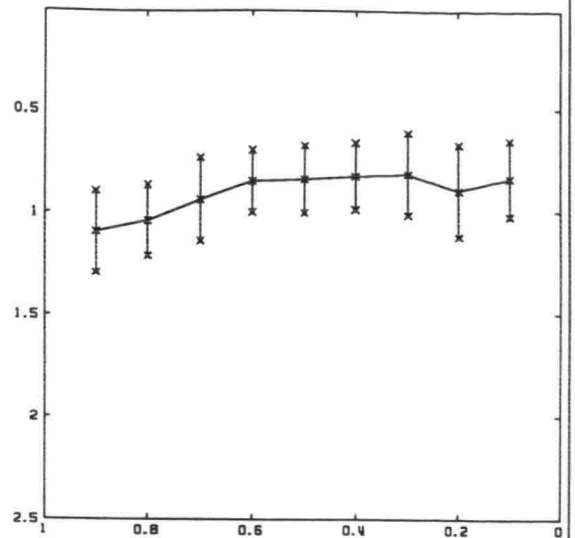
WATER DEPTH IN CROSS-DIRECTION

FIG 7F

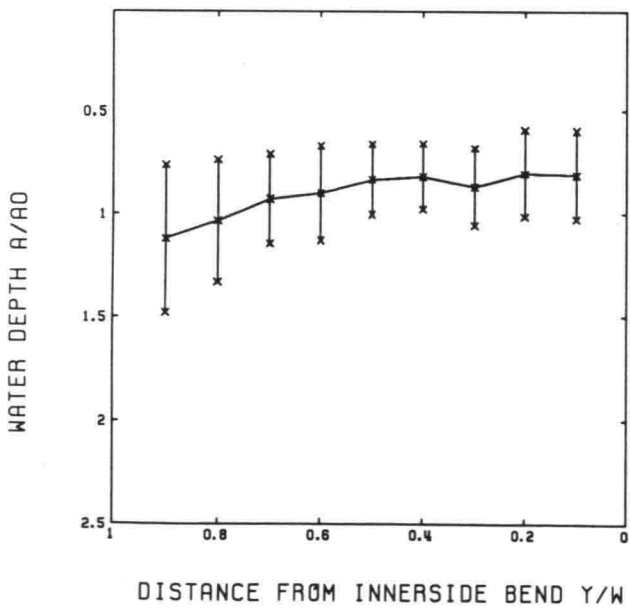
DELFT UNIVERSITY OF TECHNOLOGY



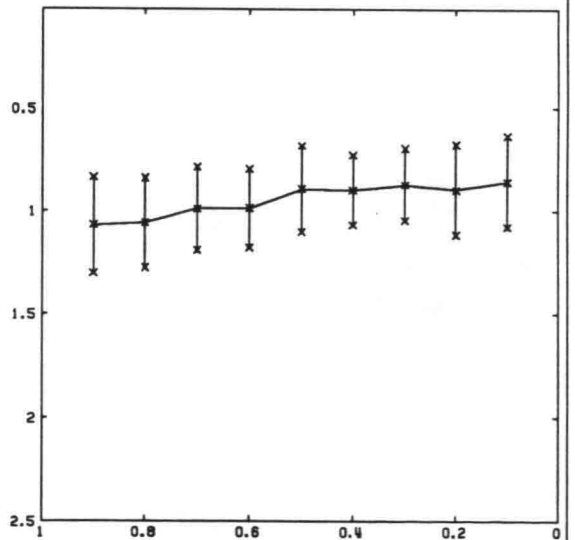
CROSS-SECTION 25



CROSS-SECTION 26



CROSS-SECTION 27



CROSS-SECTION 28

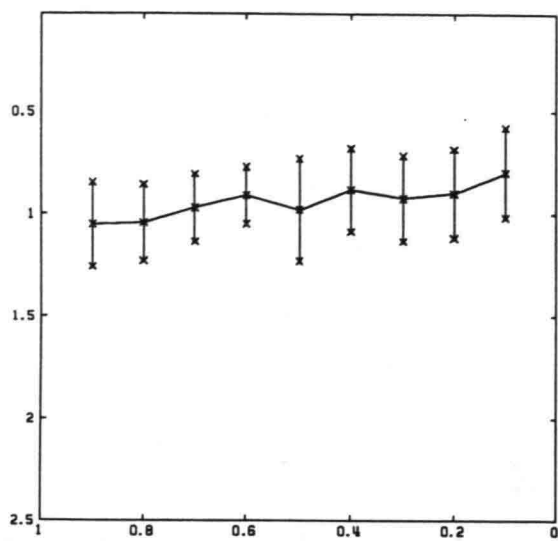
W = 0.5 M    R0 = 0.038 M

$\bar{x} \pm \sigma$  OF 23 MEASUREMENTS

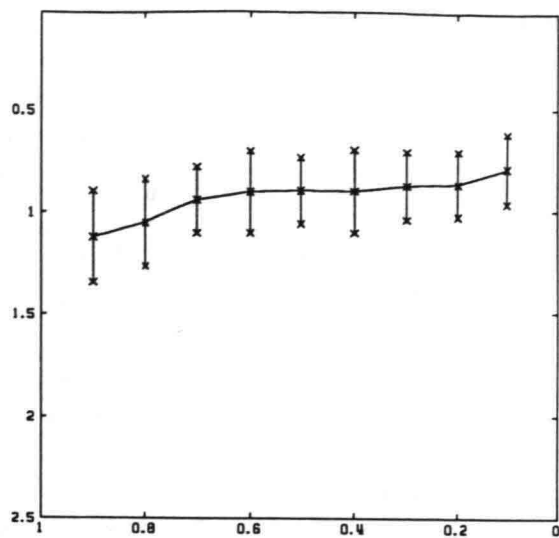
WATER DEPTH IN CROSS-DIRECTION

FIG 7G

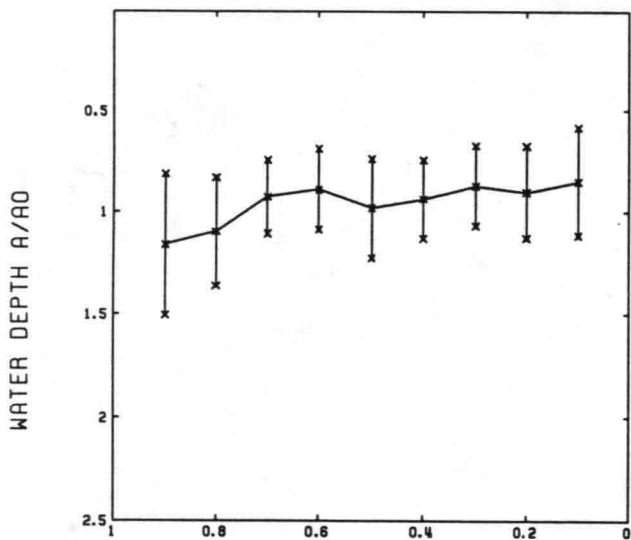
DELFT UNIVERSITY OF TECHNOLOGY



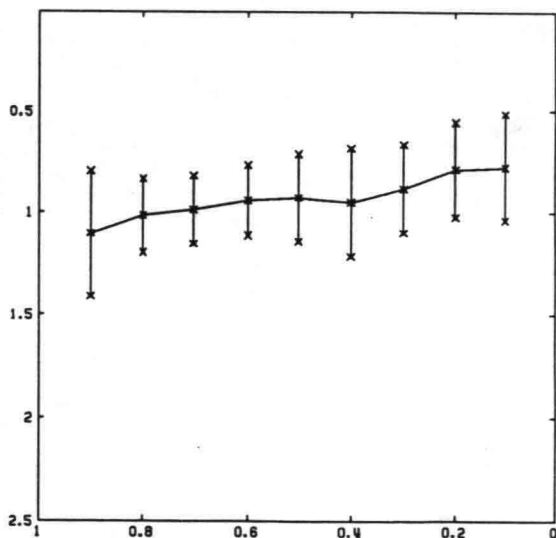
CROSS-SECTION 29



CROSS-SECTION 30



CROSS-SECTION 31



CROSS-SECTION 32

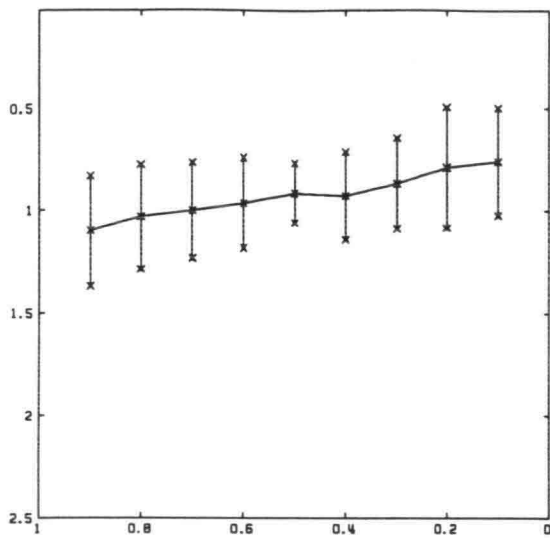
W = 0.5 M    AO = 0.038 M

$\bar{x} \pm \sigma$  OF 23 MEASUREMENTS

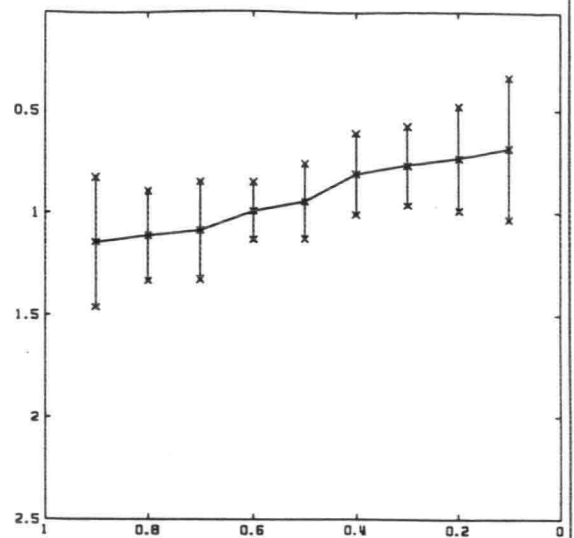
WATER DEPTH IN CROSS-DIRECTION

FIG 7H

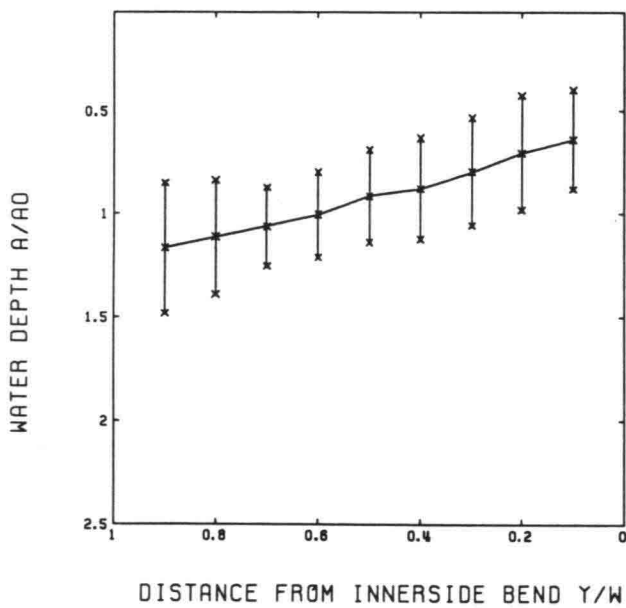
DELFT UNIVERSITY OF TECHNOLOGY



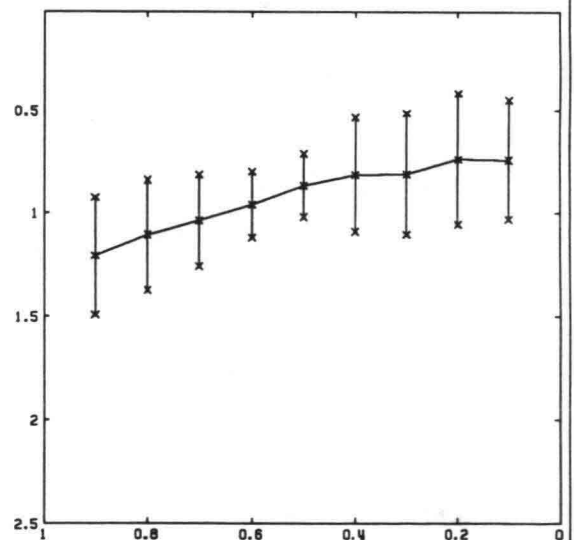
CROSS-SECTION 33



CROSS-SECTION 34



CROSS-SECTION 35



CROSS-SECTION 36

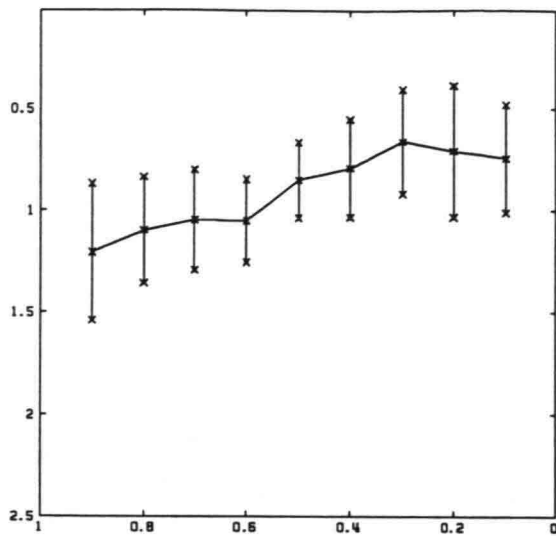
$W = 0.5 \text{ M}$      $AO = 0.030 \text{ M}$

$\pm \sigma$  OF 23 MEASUREMENTS

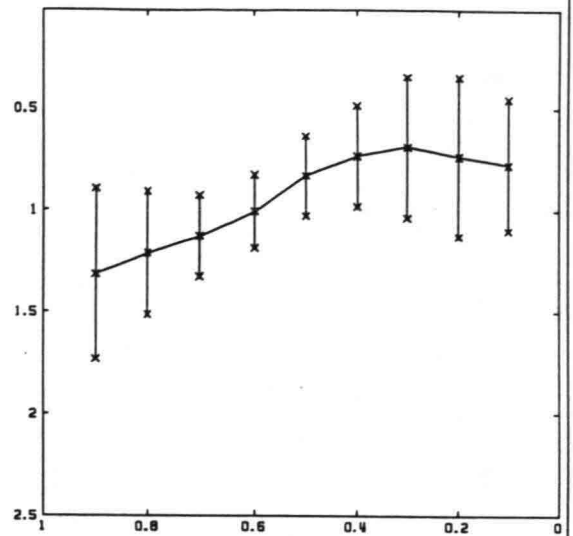
WATER DEPTH IN CROSS-DIRECTION

FIG 7I

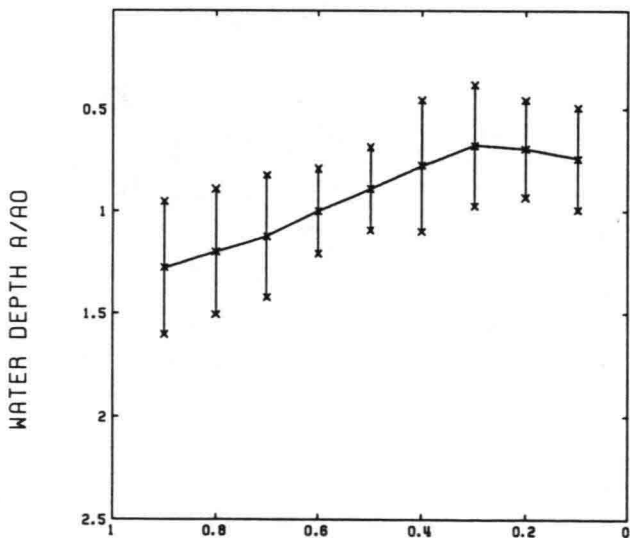
DELFT UNIVERSITY OF TECHNOLOGY



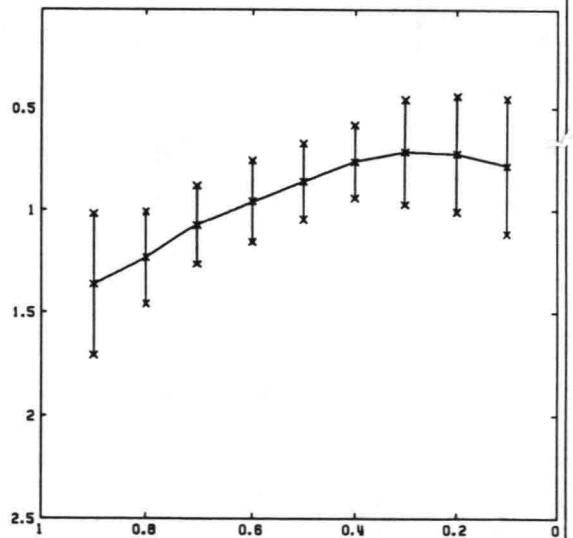
CROSS-SECTION 37



CROSS-SECTION 38



CROSS-SECTION 39



CROSS-SECTION 40

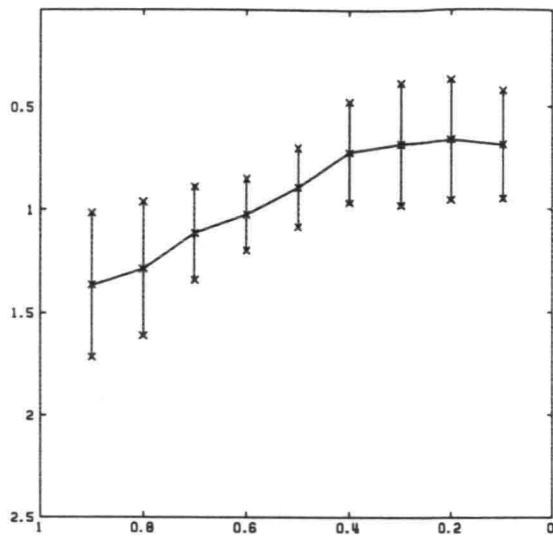
W = 0.5 M    R0 = 0.038 M

$\bar{y} \pm \sigma$  OF 23 MEASUREMENTS

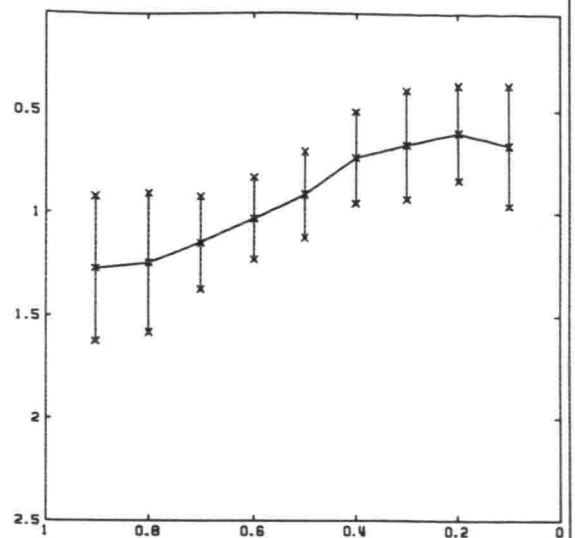
WATER DEPTH IN CROSS-DIRECTION

FIG 7J

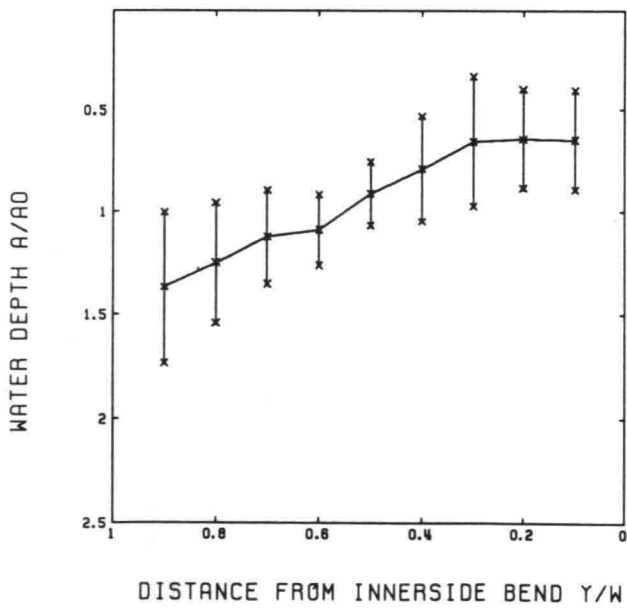
DELFT UNIVERSITY OF TECHNOLOGY



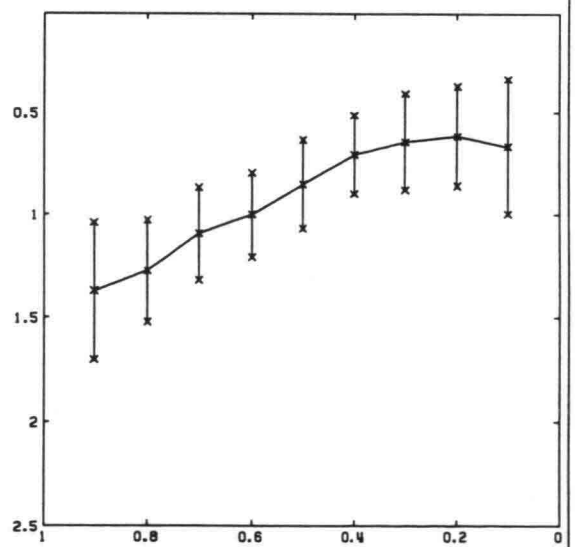
CROSS-SECTION 41



CROSS-SECTION 42



CROSS-SECTION 43



CROSS-SECTION 44

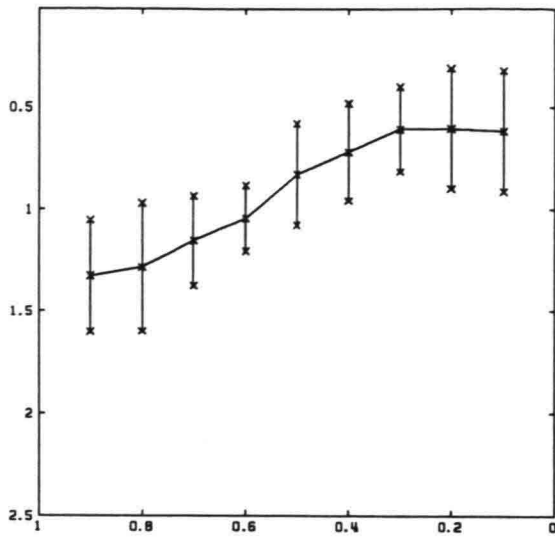
W = 0.5 M    A0 = 0.038 M

$\bar{y} \pm \sigma$  OF 23 MEASUREMENTS

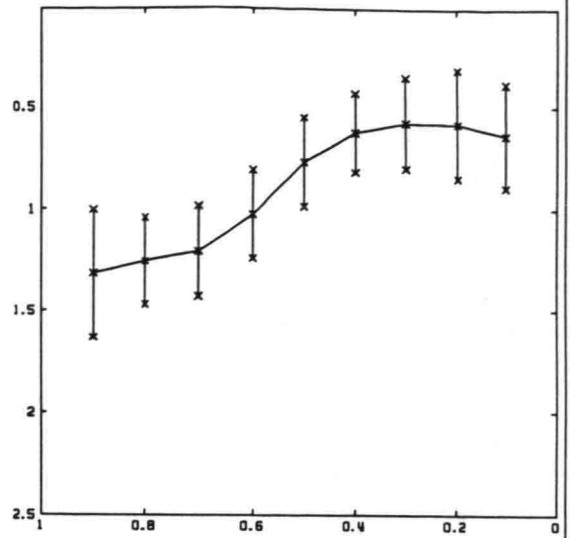
WATER DEPTH IN CROSS-DIRECTION

FIG 7K

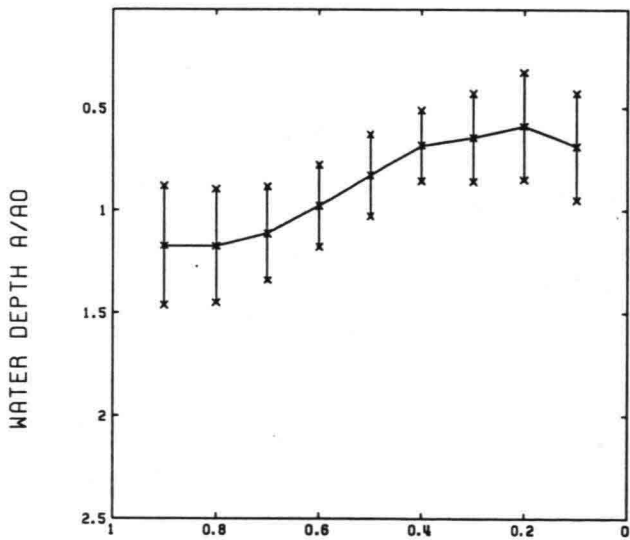
DELFT UNIVERSITY OF TECHNOLOGY



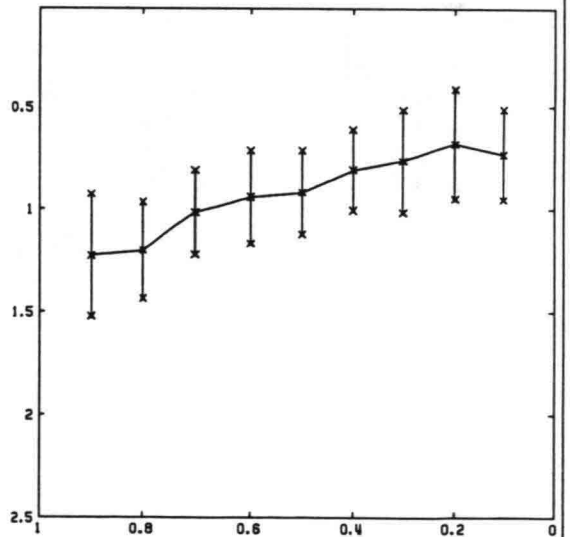
CROSS-SECTION 45



CROSS-SECTION 46



CROSS-SECTION 47



CROSS-SECTION 48

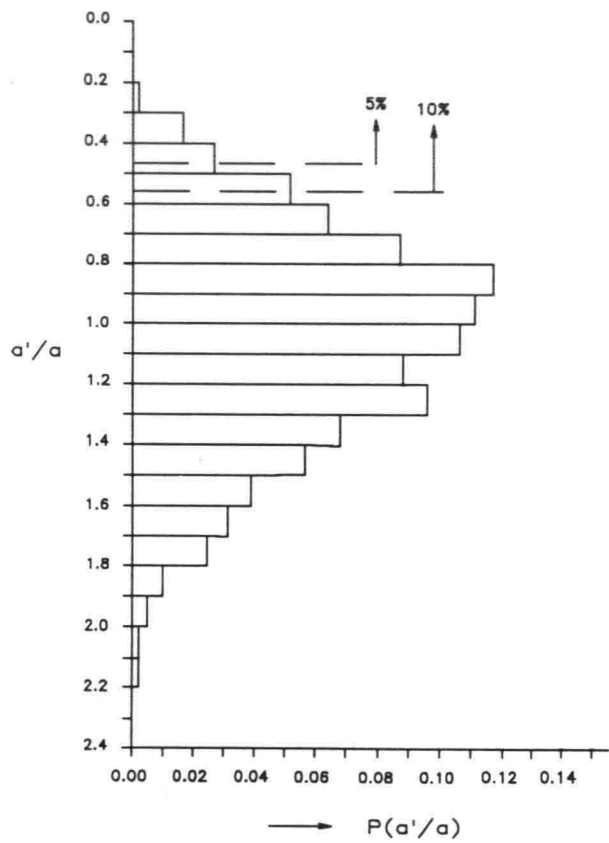
W = 0.5 M    R0 = 0.038 M

$\bar{x} \pm \sigma$  OF 23 MEASUREMENTS

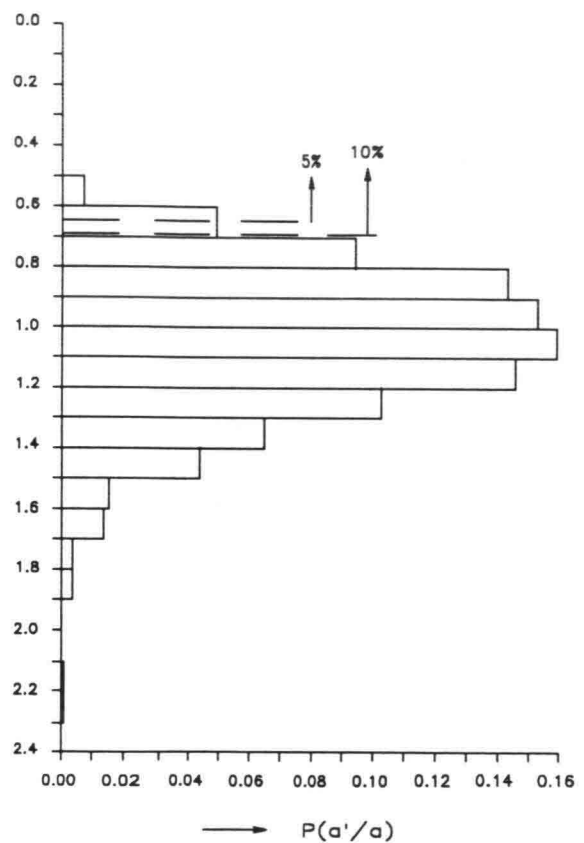
WATER DEPTH IN CROSS-DIRECTION

FIG 7L

DELFT UNIVERSITY OF TECHNOLOGY



CROSS-SECTION 1 TO 5



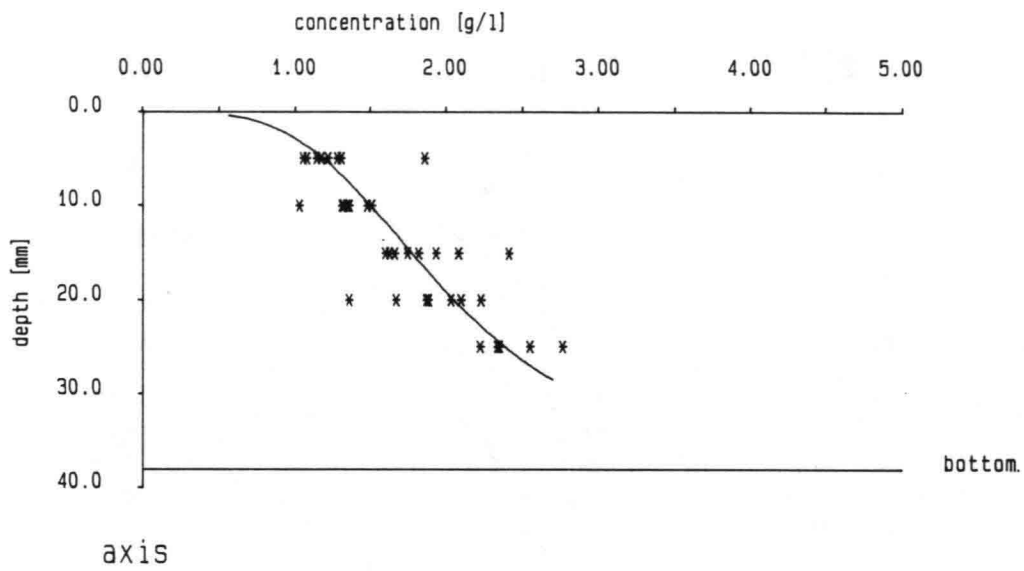
FLUME AXIS

$a'$  local water depth  
 $a$  ensemble mean local water depth

PROBABILITY DISTRIBUTION OF BED LEVEL

FIG. 8

DELFT UNIVERSITY OF TECHNOLOGY



CONCENTRATIONS AT CROSS-SECTION 1  
AND CURVE FIT BY ROUSE PROFILE

FIG. 9

